Interaction between RAGE isoforms and S100A4 in Systemic Sclerosis

2nd semester project, International Bachelor in Natural Sciences

Supervisor: Signe Vedel Borchert

Group 9:
Abia Amin, aamin@ruc.dk, 67837
Elina Kayrouz, kayrouz@ruc.dk, 73184
Irina Herrera, herrera@ruc.dk, 73159
Maya Svane, mebs@ruc.dk, 73147
Sara Angelucci, angelucci@ruc.dk, 73156
Teodora-Andreea Grasu, teodoraand@ruc.dk, 74512

May 19, 2022

Abstract

Systemic Sclerosis (SSc) is an autoimmune disorder carrying high morbidity and mortality. The main prominent finding and distinctive sign of SSc and chronic inflammation is fibrosis. Fibrosis is characterized by the activation of fibroblasts, accumulation of ECM, and the infiltration of inflammatory cells. Additionally, inflammation plays a critical role as an initiator of the progression of the disease. Recent evidence shows that patients affected by SSc have an upregulation of the S100A4 protein in their skin. The S100A4 protein is secreted at inflammatory sites and has a role in cell motility, autophagy, invasion, ECM remodeling, and angiogenesis. Under physiological conditions, S100A4 is present inside the cells, but upon exposure to stress or tissue damage, it is released into the extracellular environment. When extracellularly expressed, S100A4 interacts with a specific domain of RAGE, promoting MAPK (ERK) phosphorylation and activation of the transcription factor, NF-κB. This study explores the interaction between extracellular S100A4 and RAGE by experimental procedures, assuring the research question: What is the interaction site by which S100A4 binds to RAGE? To answer this research question, an HCT-116 Dual cell line was transfected to integrate two plasmids coding for RAGE isoform 1 and RAGE isoform 3, respectively. It was hypothesized that S100A4 is capable of binding and thereby signaling through a specific sequence being part of RAGE isoform 1 but not RAGE isoform 3. After establishing clones expressing RAGE, a SEAP assay was conducted to test the responsiveness of the cells' to S100A4. The results showed that both HCT-116 Dual RAGE 1 and HCT-116 Dual RAGE 3 were unresponsive to S100A4 being induced. As evidence suggests the opposite, further research is needed to fully understand the mechanism by which S100A4 interacts and binds to RAGE.

Contents

1 Abbreviations **5**

2 Introduction **6**

3 Background **8**
3.1 Systemic sclerosis 8
3.2 Inflammation 8
3.2.1 Cytokines and Growth factors 8
3.2.2 DAMPs and their interaction with PRRs 9
3.2.3 RAGE 10
3.3 Fibrosis 11
3.3.1 Fibroblasts and myofibroblasts 11
3.3.2 Extracellular matrix 12
3.4 S100A4 13
3.4.1 Intracellular functions of S100A4 13
3.4.2 Extracellular function of S100A4 13
3.4.3 Interaction of S100A4 with RAGE 14
3.5 NF-κB and MAPK (ERK) 14

4 Methodology **17**
4.0.1 Cell line 17
4.0.2 Transfection 18
4.0.3 Plasmids 18
4.0.4 Reporter Genes 19

5 Materials and methods **21**
5.1 Cell cultures 21
5.2 Transfection 21
5.3 SEAP assay 22

6 Results **24**
6.1 SEAP assay 24
6.2 Transfection of HCT-116 Dual cells 26
6.3 Selection of HCT-116 Dual RAGE clones 28
6.4 The ability of S100A4 to stimulate HCT-116 Dual RAGE 1 and HCT-116 Dual RAGE 3 30

7 Discussion **32**

8 Conclusion **37**

9 Perspective **38**

10 References **40**

11 Appendices **47**
11.1 SEAP assay 47
11.2 Components for induction of SEAP 49
11.3 SEAP experiment 50

1 Abbreviations

DAMP - Damage-associated molecular patterns
DNA - Deoxyribonucleic acid
ECM - Extracellular matrix
GFP - Green fluorescent protein
GOI - Gene of interest
MAPK (ERK) - Mitogen-activated protein kinase, extracellular signal-regulated kinase
mCherry - Red fluorescent protein
MEK - Mitogen-activated protein kinase kinase
NF-κB - Nuclear factor kappa B
PRR - Pattern recognition receptor
RAF - Rapidly accelerated fibrosacroma
RAGE - Receptor for Advanced Glycation Endproducts
RAS - Rat sarcoma virus
SEAP - Secreted embryonic alkaline phosphate
SSc - Systemic Sclerosis/Scleroderma
TGFβ - Transforming growth factor β

2 Introduction

Systemic sclerosis (SSc) is an autoimmune disease that attacks and damages healthy tissue, resulting in high collagen production and therefore physical changes in the skin's texture and appearance. Thus, negatively influencing many parts of the human body. Fibrosis is a pathological feature of the inflammatory disease that leads to scarring of the skin and internal organs, causing severe and at times life-threatening complications in patients with SSc. According to an article written by Dr. Allanore, et. al., 2015 [1]:

"Intractable progression of vascular and fibrotic organ damage accounts for chronic morbidity and high mortality. " [1].

The progression of successful fibrosis treatments has been found to be quite challenging. Fibrosis arises from inflammation and extracellular matrix (ECM) formation, which are important components of the body's reaction to injury and the healing process. For efficient treatment, therapy needs to address pathological inflammation and ECM production without interfering with the normal process of wound healing and matrix turnover; which is yet to be achieved [6]. In recent years, scientists discovered that S100A4, a damage-associated molecular pattern (DAMP) molecule, may play a significant role in fibrotic diseases and researchers have identified S100A4 as a potential therapeutic target [9]. S100A4 is released during inflammation and promotes ECM remodeling, contributing to fibrosis development, which becomes pathological under chronic inflammation [6, 9]. S100A4 is acting through different receptors, including Receptor for Advanced Glycation Endproducts (RAGE) and mediates downstream signaling through the RAS-RAF-MEK-ERK (MAPK(ERK)) pathway [26]. Therefore, being the aim of this project to investigate the interaction between S100A4 and RAGE in order to gain a deeper knowledge of the function of S100A4.

Thus, ensuring the research question of this project:
What is the interaction site by which S100A4 binds to RAGE?

Accordingly, the hypothesis is:
S100A4 is capable of binding and thereby signaling through a specific sequence being part of RAGE isoform 1 but not RAGE isoform 3.

To investigate if the sequence on RAGE isoform 1 is required for S100A4 binding, two plasmids encoding for RAGE isoform 1 (Plasmid M61) and RAGE isoform 3 (Plasmid M83), respectively, will be integrated into the genome of HCT-116 Dual cells by transfection to establish two different RAGE-expressing cell lines. Thereafter, a secreted embryonic alkaline phosphate (SEAP) reporter assay will be conducted to test if the

RAGE-expressing cell lines have become responsive to S100A4 by measuring SEAP activity. HCT-116 Dual cells harboring RAGE isoform 1 are hypothesized to become responsive to S100A4, whereas HCT-116 Dual cells harboring RAGE isoform 3 should not be responsive to S100A4 due to RAGE isoform 3 lacking the putative sequence for S100A4 binding.

3 Background

In order to understand the development of the disease, SSc, further detail of the complex cellular and molecular mechanisms that underlie fibrosis in SSc is required.

3.1 Systemic sclerosis

SSc, or scleroderma, is an autoimmune disorder, meaning that the body is attacked by its immune system. In more detail, the immune system mistakenly targets and destroys the healthy tissue assuming that it is an infection. For SSc, this results in increased collagen production and thus, in physical changes in the skin's texture and appearance [2]. However, it may also negatively affect the blood vessels, digestive tract, and internal organs. Even though there is not any cure for SSc, some treatments are available so that patients can have a better quality of life with slow progression of the disease and easier symptoms [3]. In short, inflammation and fibrosis play crucial roles in SSc and lead to severe damage and failure of multiple organs including the skin, joints, lungs, heart, tendons, gastrointestinal tract, blood vessels, and kidneys. Hence, the disease can cause several health issues and even become life-threatening [4].

3.2 Inflammation

SSc is a cause of chronic inflammation, leading to progressive fibrosis of the skin and internal organs. In order to fully comprehend the components that entail symptoms caused by autoimmunity, a closer look at the inflammatory responses is required.

When epithelial and endothelial cells are damaged due to autoimmunity, they release inflammatory mediators that activate an antifibrinolytic coagulation cascade, which initiates blood-clot production and formation of provisional ECM [5]. It has been found that continuous inflammatory trigger is crucial for the activation of the wound-healing mechanism that leads to fibrosis. Thus, disposal of the inflammatory trigger is the most straightforward way to reduce and eventually stop the progression of tissue remodelling. Allowing the normal tissue structure to be restored after injury, since, proper wound healing first occurs when inflammation is controlled [6].

3.2.1 Cytokines and Growth factors

The cause of SSc remains unknown, however, the production of growth factors, specifically cytokine production and release, has been observed to be a vital trigger of immune response and autoantibody production, collectively leading to microvascular

damage, inflammation, and fibrosis [7].

Growth Factors are protein molecules produced by the body that promote cell growth by mitogen production and function as regulators of cell division and cell survival. They attach to receptors on the cell surface, causing cellular proliferation and/or differentiation when activated [8]. The subtype of growth factors, cytokines, cover multiple proteins and peptides that act as mediators under the immune response. Cytokines thereby inflect functional activities of tissues or cells under normal or pathological conditions [7].

An example of an important cytokine involved in inflammation and fibrosis is the transforming growth factor-beta (TGF-β), a type of cytokine that controls cellular differentiation, proliferation, and other functions in most cells. TGF-β is a central mediator of fibrosis and acts as a growth factor that controls cellular differentiation and stimulation of fibroblasts into myofibroblasts [51].

3.2.2 DAMPs and their interaction with PRRs

Upon tissue injury or cellular stress during inflammation, DAMPs molecules are released and play an important role in the pathogenesis of autoimmune diseases such as SSc [10].

DAMPs are considered endogenous danger signals triggering the innate immune system to produce a potent inflammatory response during non-infectious inflammation. During inflammation, DAMPs are either released into the extracellular space or intracellular space by a stimulus, thereby originating from different sources, including both intracellular proteins and extracellular proteins [10]. When secreted to the extracellular space, DAMPs bind to immune cells by specific receptors and consequently facilitate the activating of innate immunity, cell differentiation, death, or the release of inflammatory mediators, thus amplifying the inflammatory response [9].

The activation of the innate immune system occurs through DAMPs interacting with pattern recognition receptors (PRRs). PRRs are crucial components of the innate immune system. The main function of PRRs is to recognize microbes or tissue damage by interacting with molecules such as DAMPs, and initiate inflammatory signaling pathways to induce innate immunity. In addition, DAMP-PRR interaction leads to the release of inflammatory cytokines [10].

3.2.3 RAGE

One receptor being categorized as a PRR is RAGE, because of its ability to bind to a large variety of ligands [11]. It is characterized by having multifarious isoforms [28].

RAGE is identified as a transmembrane, multiligand, and more specifically a DAMP receptor, and is a binding site for a wide range of ligands such as different DAMPs, including some S100 proteins [12]. When ligands bind to RAGE on endothelial cells, smooth muscle cells, monocytes, and macrophages, it activates several different signaling pathways. The cell response is heterogeneous, depending on the specific ligand and cell type involved in the interaction [13].

The inflammatory response that DAMP-RAGE interaction entails ranges from high to none. The DAMPs that have been found more effective in RAGE activation are the ones capable of oligomerization. Oligomers of ligands are capable of recruiting RAGE receptors and inducing their congregation on the cell surface [11].

3.2.3.1 RAGE: Chemical structure and mechanism

A mature RAGE consists of an extracellular part, containing 314 amino acids, a transmembrane spanning helix, which consists of 27 amino acids, and a short cytosolic domain, containing 41 amino acids. A mature RAGE thereby entails a total of 382 amino acids. Furthermore, it should be noted that RAGE forms oligomers on the surface of the cell [28].

The transmembrane form of RAGE contains both intracellular and extracellular domains. The intracellular domain is necessary for both the interactions with cytoplasmic proteins, as well as multifarious forms of RAGE signaling, including the activation of the MAPK (ERK) signaling pathway and the nuclear factor kappa B (NF-κB) [40].

A multiligand RAGE receptor consists of three extracellular domains: V1, containing an N- terminal, C1, and C2 (see figure 1, p. 16). The V-type domain is considered to be essential for ligand binding, and C-type domains play a crucial role in stabilizing the V-domain. RAGE binds a variety of ligands and displays a preference for aggregation-prone ligands as well as those undergoing post-translational modification. Furthermore, the RAGE receptor serves as a scaffold for the initiation of signal transduction. RAGE is attached and secured to the cell membrane by its transmembrane domain. As a result of RAGE-ligand interaction, a cascade of metabolic changes is induced, causing alterations in the expression of key cell proteins and contributing to the production of inflammatory cytokines [41].

3.3 Fibrosis

Fibrosis is a prominent pathological finding and a distinctive sign or consequence of SSc and chronic inflammation [16].

In fibrosis, various tissues become overgrown, hardened, and scarred due to excess collagen deposition in the ECM. The basic mechanisms of fibrogenic responses show similarities to normal wound healing, however, the wound healing process has gone awry, in which cells producing ECM become overly active, thereby forming excess ECM, causing substantial scar formation and resulting in an architectural remodeling process in all tissues and organs [17].

In most cases, fibrosis is initiated by cell death that is driven by various injurious agents and mechanisms. Damage to the tissue triggers an inflammatory response in which local immune cells, primarily macrophages, become activated and diverse sets of blood cells enter the injured areas [17]. The activated local immune cells produce a large variety of growth factors and cytokines such as TGF-β. These cytokines convert the epithelial and endothelial cells in the organs into fibroblasts via their receptors on the cell membrane, leading to the activation of the epithelial and endothelial cells. These activated cells cause the production of collagen and ECM, resulting in the formation of fibrosis [18]. Furthermore, these components can regulate the development of fibrosis and may be therapeutic targets for the treatment of fibrosis [19].

To summarize, there are two major contributors to fibrosis, the activation of epithelial and endothelial cells by cytokines, and the deposition of a large amount of ECM molecules.

3.3.1 Fibroblasts and myofibroblasts

Fibroblasts are the most prevalent type of connective tissue cells [21], and the main source of the production of ECM components, primarily collagen. Fibroblasts release and regulate cytokines in response to changes like a mechanical stretch, which can result in increased TGF-β production [20]. Furthermore, these cells produce many ECM structural proteins, adhesive proteins, and ground substances, all of which are fundamental to maintaining the ECM. Fibroblasts also play an essential role in wound healing, inflammation, angiogenesis, and pathological and physiological tissue fibrosis [21]. By definition, angiogenesis is the formation of new blood vessels, which is a process

that is strongly associated with pulmonary fibrosis that can develop into organ fibrosis [9].

Fibroblasts can be activated to form myofibroblasts by differentiation (see figure 1, p. 16) [19]. These cells are involved in the inflammatory response to injury, where they serve to condense the size of wounds [23]. Hence, these cells only appear after cardiac injury and are not present in healthy cardiac tissues [20]. Upon injury, myofibroblasts will migrate to the site of injury, where they initiate cytokine production, thereby amplifying the inflammatory response [18]. The activation of fibroblasts is therefore vital in wound healing, however, in some cases, their activation becomes uncontrolled, resulting in a pathological fibrotic response as seen in patients with SSc [19].

3.3.2 Extracellular matrix

Chronic inflammation and repair can trigger a disproportionate accumulation of ECM components, which leads to the formation of an enduring fibrotic scar [5]. The ECM thereby plays a vital role in fibrosis.

The ECM is a dynamic network composed of an arrangement of multidomain macromolecules organized in a cell/tissue-distinct manner. Components of the ECM join together to form a structurally stable compound, contributing to the mechanical properties of tissues. Additionally, growth factors and bioactive substances are also stored in the ECM. It holds a major role and is of vital importance in determining and controlling the most essential roles and characteristics of cells such as proliferation, adhesion, migration, polarity, differentiation, and apoptosis [25].

The ECM's biochemical characteristics allow cells to sense and interact with their extracellular environment through a variety of signal transduction pathways. The chemical cues are provided by ECM components, especially the adhesive proteins such as fibronectin, integrin, and non-integrin receptors, along with growth factors and associated signaling molecules [25].

The ECM consists of many components, including an array of different types of proteins, collagen being one of the most significant [58].

Collagen is the main structural protein in the ECM. It provides tensile strength, balances cell adhesion, supports chemotaxis and migration, and directs tissue development. Collagens are thereby a way to quantify the balance between the formation and degradation of tissue which is of relevance when dealing with SSc [58].

3.4 S100A4

A compound having a notable effect in driving fibrosis is S100A4 [26]. The protein S100A4, also known as fibroblast-specific protein 1, is included in the S100 family of small calcium-binding proteins and is a multi-receptor ligand [9, 26]. In humans, this protein is encoded by the S100A4 gene. As part of its biological functions, S100A4 plays a role in angiogenesis, cell differentiation, apoptosis, motility, and invasion. Under different pathological conditions, S100A4 can also trigger inflammatory processes and promote the release of cytokines and growth factors. S100A4 exhibits both intracellular and extracellular activities [26].

3.4.1 Intracellular functions of S100A4

The expression of intracellular S100A4 is associated with healthy conditions. The S100A4 gene expression contributes to cell migration, apoptosis, and stemness maintenance. The vast majority of the protein in the cell is found within the cytoplasm, although some are also found in the nucleus [26].

3.4.2 Extracellular function of S100A4

In case of stress or tissue damage, S100A4 is secreted by the cell via diffusion. In the extracellular environment, S100A4 stimulates inflammatory processes and causes various molecules to be produced, such as cytokines, growth factors, and ECM proteins. Regarding S100A4's influence on immune regulation, its extracellular activity is of particular importance, as the extracellular form of S100A4 is known to activate pro-inflammatory pathways and is an established stimulator of cytokine production. Thus, there is a dual effect of the extracellular function of S100A4 in immune cells. Firstly, it affects the differentiation of immune cells of the innate and adaptive immune system, and secondly, it activates these cells to produce a variety of cytokines. Cytokines are secreted as a result of cells from the innate and adaptive immune systems being activated by S100A4 [26]. Hence, the web of cytokines is responsible for the regulation of the immune response [9].

Furthermore, the S100A4 protein is being considered an effective DAMP protein by studying its extracellular oligomeric form, its specific cell surface receptors (RAGE, Toll-like receptor 4, Epidermal growth factor receptor), and its high affinity to activate pro-inflammatory pathways [9, 26].

3.4.3 Interaction of S100A4 with RAGE

S100A4 is an important modulator of cellular motility through its interaction with RAGE and leads to the modulation of vascular smooth muscle cells, thyroid and colon cancer cells through MAPK (ERK) signaling, and hypoxia. Current findings indicate that S100A4 binds to the hydrophobic region on the V1 domain of RAGE. In a recent study, data presented demonstrated that both extracellular treatment and intracellular overexpression of S100A4 can cause RAGE-dependent inhibition of autophagy via the β-catenin pathway [26]. During autophagy, unnecessary or dysfunctional components of the cell are removed. As a result, cellular components are degraded and recycled in a controlled manner. Furthermore, autophagy dysregulation has now been recognized as a factor in the progression of fibrosis [9]. The same study also indicated that the angiogenic activity of S100A4 is mediated through S100A4's interaction with RAGE [26]. In inflammatory diseases, the response to normal pathological stimuli is enhanced in respect to promoting angiogenesis, which is a required part of inflammatory processes and may contribute to tissue growth [29].

Furthermore, researchers have verified that extracellular S100A4 interacting with RAGE, promotes MAPK (ERK) phosphorylation and activates the NF-κB axis. Indirectly and directly, activation of NF-κB leads to the release of pro-fibrogenic and pro-proliferative factors, which lead to the development of fibrosis [9].

3.5 NF-κB and MAPK (ERK)

In order to fathom the downstream effect of S100A4 binding to RAGE, an understanding of both the MAPK (ERK) signaling pathway, as well as NF-κB is necessary (see figure 1, p. 16).

The MAPK (ERK) pathway is composed of a small guanine nucleotide-binding protein (RAS) and three protein kinases (RAF, MEK, ERK). Kinases are enzymes that catalyse the transfer of phosphate groups from donor molecules to acceptor molecules. The MAPK (ERK) pathway is initiated by the binding of a ligand to a cell surface receptor. The binding allows for a RAS protein, a small GTPase, to swap a guanosine diphosphate (GDP) molecule for a guanosine triphosphate (GTP) molecule, flipping the "on/off switch" of the pathway. During RAS's active state, it activates a protein kinase known as a mitogen-activated kinase kinase kinase (MAPKKK), also known as RAF [30].

RAF (MAPKKK), a cytosolic protein kinase, facilitates the phosphorylation of the second protein kinase in the cascade, known as MEK (MAPKK). MEK has a dual-specificity for tyrosine and serine/threonine residues, a function critical for the

activation of the final enzyme in the cascade, and ERK (MAPK). To activate ERK, double phosphorylation of a tyrosine residue and an almost-adjacent threonine residue is required. As a result, ERK is able to function as an enzyme and translocate to the nucleus, where it phosphorylates and activates transcription factors [30].

A transcription factor activated by the MAPK (ERK) signaling pathway is NF-κB. NF-κB is a family of inducible transcription factors that are known to regulate a number of genes involved in various immune and inflammatory responses. Post activation, NF-κB enters the nucleus and initiates gene expression which induces the transcription of various genes, hence NF-κB becomes a regulator of inflammation. Accordingly, NF-κB targets genes involved in the progression and development of inflammation. Furthermore, the expression of numerous pro-inflammatory genes that NF-κB induces, includes those encoding for chemokines and cytokines [31]. Thus, NF-κB mediates the upregulation of pro-inflammatory cytokines [32]. NF-κB also targets inflammation by regulating cell proliferation, apoptosis, morphogenesis - a biological process that generates tissue organization, shape, and differentiation [27, 31].

An example is the innate immune cells that are regulated by NF-κB. Innate immune cells express PRRs, like RAGE, which recognizes DAMPs, like S100A4. An important signaling event in PRRs is the activation of the canonical NF-κB pathway, whose transcriptional activation is responsible for inflammatory cytokines, chemokines, and other mediators in various innate immune cells [31]. Under normal conditions, NF-κB gets activated in cells by receiving the appropriate stimuli, and in response to its activation, it upregulates the transcription of its target genes. After a series of regulatory mechanisms, NF-κB returns to an inactive state, hence it being an inducible transcription factor. The activation of NF-κB may be impaired by different types of molecular alterations. This may result in dysregulated expression of genes controlled by NF-κB, including genes that regulate apoptosis, cell cycle control, adhesion, or migration [33]. Consequently, dysregulated NF-κB activation is associated with playing a vital role in the pathogenesis of several inflammatory diseases, including SSc [31].

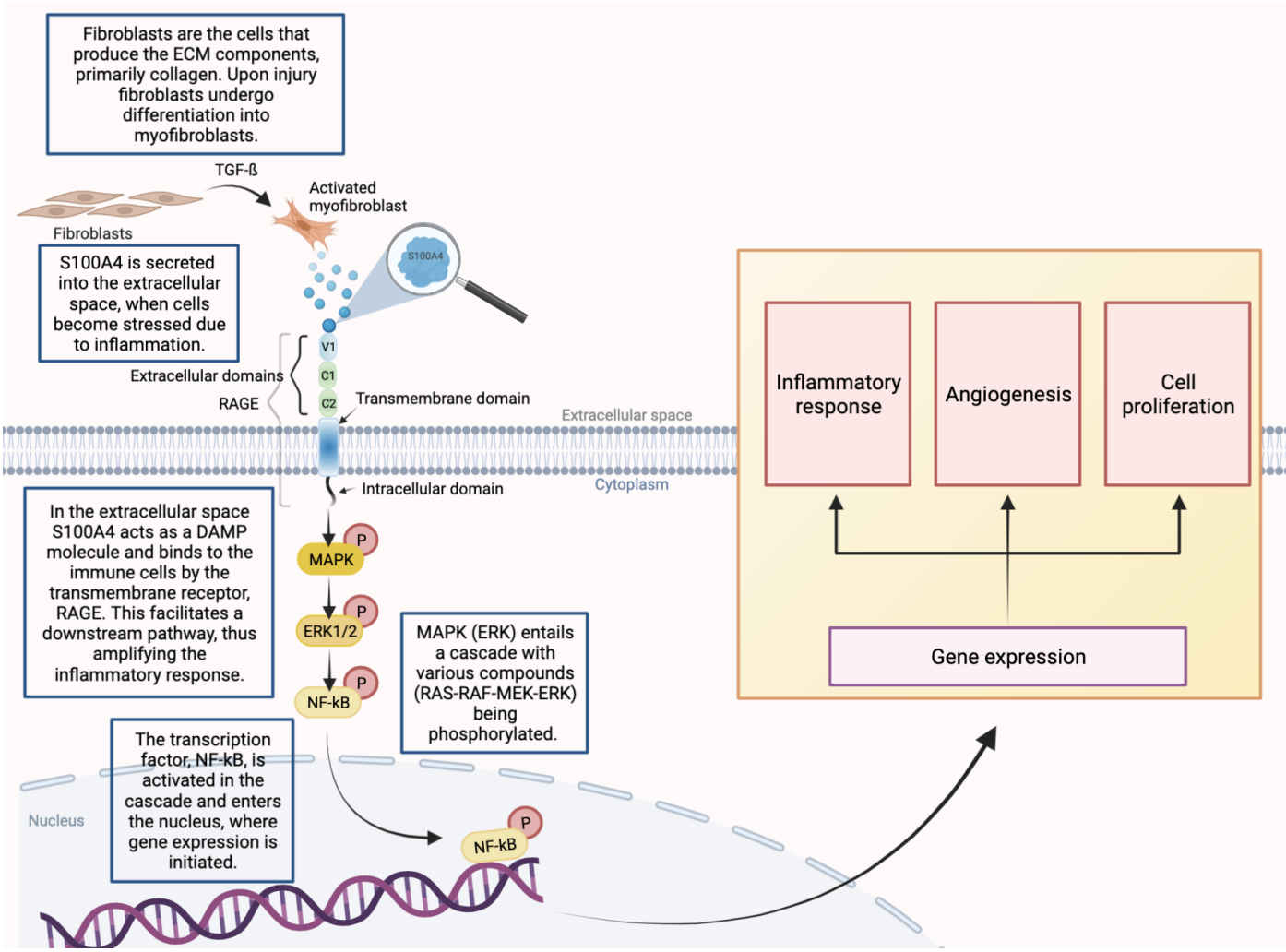

Figure 1: Fibroblasts are differentiated into myofibroblasts, and S100A4 is secreted out by the cells to the extracellular space. The binding of S100A4 to RAGE initiates the MAPK (ERK) pathway, which consists of the phosphorylation of various compounds. The MAPK (ERK) cascade ends with the transcription factor, NF-κB, being activated and entering the nucleus, where NF-κB initiates gene expression. As a concluding point, figure 1 provides a visual summarization corresponding to the cascade of events that occur in people suffering from fibrosis. This figure was created in BioRender, inspired by [9] and [42].

4 Methodology

The major aim of the following experimental procedures is to integrate a deoxyribonucleic acid (DNA) fragment, called a plasmid, into the genome of HCT-116 Dual cells to investigate a gene of interest (GOI), which is RAGE. The transfected cells are used to investigate the interaction between S100A4 and RAGE by testing the ability of S100A4 to bind to two different isoforms of RAGE: RAGE isoform 1 and RAGE isoform 3, respectively.

In order to fathom the procedures done during the experiments, certain background knowledge of the methods in hand is needed.

4.0.1 Cell line

A cell line is a culture of cells that is permanently established [34]. Permanently established cells are defined as being unable to differentiate in postnatal life, meaning that they neither reproduce nor transform into other cells [67]. These cells can thus be cultured for an unlimited period of time, granted that the ideal medium and space are provided [34]. Cell lines are normally used for studies and laboratory work in the field of biology. There are various advantages to utilising cell lines, including cost-effectiveness, ease of use, the large number of data that can be produced due to the endless supply of material, and the ability to avoid ethical difficulties related to the use of animal and human tissue [35].

For the purpose of the project research, HCT-116 Dual cells, adherent epithelial cells that are derived from human colon cancer, will be used. The cell line has high transfection efficiency and it does not contain either RAGE or Toll-like receptor 4. When creating an artificial system by transfection to study a particular gene, it is beneficial not to have many other factors interacting. Therefore, it is favorable that the basal/endogenous levels of RAGE and Toll-like receptor 4 are low or absent, to avoid these factors interacting with S100A4 and thereby contributing to the signaling. By these parameters, it becomes easier to interpret the results because it can be trusted to a certain extent that the effect comes from the integrated RAGE. On the contrary, if the cells have had high endogenous levels of RAGE, it would not have been possible to distinguish whether S100A4 signals through the endogenous RAGE or the integrated RAGE [53].

By means of the mentioned, this cell line was chosen to be utilised to study the interaction between S100A4 and the integrated RAGE.

4.0.2 Transfection

Transfection refers to the process of artificially introducing foreign nucleic acids [either DNA or ribonucleic acid (RNA)] into cells, utilising means other than viral infection. Transfection is therefore a powerful analytical tool used to alter the expression and properties of cells by altering the host genome, allowing the study of gene function and protein expression or blockage in the context of the cell. By this method, a particular cell population with a more uniform level of gene expression is established, creating a system that can be utilised during long-term experimental work. However, it is of great importance that the nuclear material is not only introduced in the cell but also delivered to the nucleus to be integrated into the host genome when creating a stable cell line. Furthermore, to select the stable clones expressing the GOI, a positive biomarker, such as an antibiotic, can be utilised. In addition, introducing proteins into cells with easily detectable markers and other alterations allows researchers to investigate promoter and enhancer sequences as well as protein-protein interactions. Thus, the main purpose of transfection is to specifically enhance or inhibit gene expression in transfected cells. For that reason, the technique can be applied to study a variety of things such as the function and regulation of genes or gene products for producing transgenic organisms, and as a method for gene therapy [37, 38].

4.0.3 Plasmids

The two plasmid codings for the two RAGE isoforms are:

- A0070-M61: RAGE Isoform 1 – Green fluorescent protein (GFP)
- A2189-M83: RAGE Isoform 3 – Red fluorescent protein (mCherry)

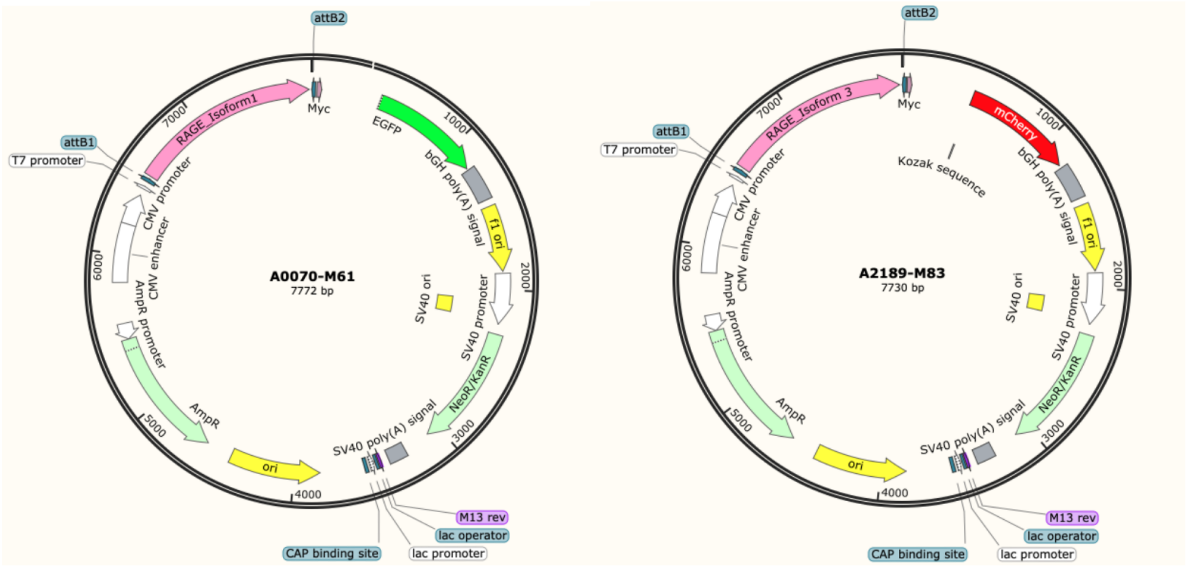

Figure 2: The left side illustrates the plasmid coding for RAGE isoform 1, and it is suspected to have a binding site for the S100A4 protein. The plasmid contains the reporter gene, GFP, and the NeoR/KanR antibiotic-resistant gene. On the right, the plasmid coding for RAGE isoform 3 is presented, and it is suspected not to have a binding site for the S100A4 protein. The plasmid contains mCherry and the antibiotic-resistant gene, NeoR/KanR.

4.0.4 Reporter Genes

Reporter genes are genes used in biological research to allow researchers to see when a GOI is expressed in cells. Reporter genes produce products that can be readily detected after transfection and can serve as markers for successfully transfected cells, as a means of regulating gene expression, or as a method for standardizing transfection efficiency [37]. In this study, there is one reporter gene per plasmid of interest.

GFP is the reporter gene expressed in the plasmid coding for RAGE isoform 1, the plasmid with a suspected binding-site for S100A4. Using DNA recombinant technology, the GFP gene is combined with the GOI, through insertion of GFP into the DNA sequence by attaching it downstream to the promoter. A cell can thereby be transformed with this newly created GFP-tagged DNA and studied for gene expression. Since both the GOI as well as GFP are on the same piece of DNA, they will be transcribed together into mRNA. When the RNA is translated into protein, it will contain both GFP and GOI. Therefore, detecting the presence of the gene would be simple, since GFP is reporting it. If the cell fluoresces green under a fluorescence microscope, the GOI is also supposedly being expressed [54].

mCherry is the reporter gene used in the other plasmid coding for RAGE isoform

3, the plasmid with no suspected binding site for S100A4. mCherry is a fluorescent protein, which functions the same way as GFP, but fluoresces red under a fluorescence microscope instead [55].

The purpose of reporter genes is, therefore, to be able to identify cells that have had the plasmid inserted by transfection. In this way, the clones, groups of cells that contain the plasmid, can be isolated [38].

SEAP is a reporter commonly used to study promoter activity or gene expression. Due to alkaline phosphatases usually being membrane-bound, they are not secreted. This recombinant reporter gene can be constitutively expressed and dynamically released from transfected cells [38]. SEAP serum assay has been used in measuring promoter and transcription factors activation and inhibition [59]. In this study, SEAP is the reporter gene for stimulating RAGE. The HCT-116 Dual cell line has been modified from Invivogen, thus the cells express SEAP. Provided that RAGE is expressed and sits in the cell membrane, certain ligands, substances that work through RAGE, as S100A4 should give a stimulus in the cell to initiate the MAPK (ERK) cascade that activates NF-κB, thereby initiating the expression of SEAP. SEAP is the reporter gene that specifically expresses if a ligand initiates the NF-κB pathway, which S100A4 does. SEAP is only activated in case of sufficient stimulation of RAGE because RAGE is the upstream receptor to the NF-κB pathway. Hence, SEAP is used to detect whether S100A4 has been able to bind to RAGE or not. SEAP is detected by giving the cells a specific medium, called HEK detection, that contains a substract that SEAP hydrolyses to produce a purple/blue colour that can be easily detected with the naked eye or measured with a spectrophotometer [57, 59].

5 Materials and methods

5.1 Cell cultures

HCT-116 Dual cells (HCT-116 Dual. Invitrogen. Cat. No. hctd-nfis) were cultivated in Dulbecco's modified Eagle's Medium (DMEM) containing 4500 mg/l glucose (ThermoFisher. Cat. No. 31966-021) supplemented with 10% Fetal Bovine Serum (FBS) (ThermoFisher. Cat. No. A3840402) and 1% penicillin streptomycin (Pen-strep) (ThermoFisher. Cat. No. 15140-122) as well as 10μg/ml Blasticidin (Invovogen. Cat. No. ant-bl-1) and 100μg/ml Zeocin (ThermoFisher. Cat. No. R250-01) and incubated at 37.5°C in a humidified atmosphere of 5% CO_2 in T75 flasks. Blasticidin and Zeocin are used for maintaining the SEAP activity in the HCT-116 Dual cells. The cells were sub cultivated twice a week. Media was removed by aspiration and the cells were washed once with 10 mL of Dulbecco's phosphate-buffered saline (DPBS) modified without Ca^{2+} and Mg^{2+} (Gibco. Cat. No. 14190-144) to remove dead cells, waste compounds, etc. The cells were trypsinized with TrypLE (ThermoFisher. Cat. No. 12604013) solution, which is an enzyme that facilitates the detachment of cells from the bottom of the plate. In order for the enzyme to catalyse the detachment of the cells, the T75 flasks were incubated at 37.5°C in a humidified atmosphere of 5% CO_2 in order to fasten the procedure. When the cells have become detached, they are resuspended in 5 ml DMEM media supplemented with FBS, Pen-strep as well as the two antibiotics (Blasticidin and Zeocin). The cells were resuspended by the use of a serological pipette to obtain a single cell suspension.

Then $1 - 1.5 * 10^6$ cells were then transferred to a new T75 flasks for further cultivation with 12 mL medium per plate.

5.2 Transfection

Day 1: 800 000 cells are seeded per well in a 6 well plate and incubated at 37.5 °C in a humidified atmosphere of 5% CO_2 overnight.

Day 2: In this part of the experiment, 2.5 μg DNA is firstly diluted into 125 μl Opti-MEM (ThermoFisher. Cat. No. 31985-070). The DNA/ Opti-MEM mixture is then incubated at room temperature for 5 minutes. 10μl of the transfection reagent, Endofectin (GeneCopoeia. Cat. No. EF013/EF014) is diluted in 115μl Opti-MEM. Using Endofectin as a transfection reagent allows the plasmids to enter the cells through the cell membrane. The diluted transfection reagent is then combined with the diluted DNA, thereby obtaining a 250 μL DNA-transfection mixture. A transfection mixture was prepared for each plasmid: one mixture containing the plasmid coding for RAGE

isoform 1, and one mixture containing the plasmid coding for RAGE isoform 3. The DNA-transfection mixture for each plasmid is then incubated for 20 minutes, allowing DNA-transfection reagent complexes to form. The DNA-transfection reagent complexes are then added drop by drop directly into the cell culture medium. The cells are then incubated overnight at 37.5 °C in 5% CO_2.

Day 3: The cells are washed twice with 4 mL DPBS without Ca^{2+} and Mg^{2+} (Gibco. Cat. No. 14190-144), whereafter the cells are detached from the bottom of the 6 well plate by utilising 200 μL trypsin (TrypsinLE solution. Gibco. Cat. No 12604-013), followed by incubating the plate at 37.5 °C in 5% CO_2. The cells are then resuspended until they have a single cell suspension and 2 mL of the mixture containing cells is added to a 10 cm cell culture dish. 10μl of DPBS without Ca^{2+} and Mg^{2+} is then added to the culture plate. The culture plate is incubated overnight in order to let the cells adhere to the bottom of the plate.

Day 4: The old medium is removed, and then a new medium, containing selective antibiotics (1 mg/ml G418 (neomycin)) is added to the culture plates, in order to kill the untransfected cells.

The selection was continued over four weeks, where the medium was changed 3x per week during the first couple of weeks, and 2x per week during the remaining time.

5.3 SEAP assay

HEK detection (Invivogen. Cat. No. hb-det2) is a cell culture medium utilised as a method to observe SEAP expression. HEK detection contains a substrate that SEAP hydrolyses to produce a purple/blue colour that can be easily detected with the naked eye or measured at an optical density (OD) of 620 nm with a spectrophotometer. Detection of SEAP, therefore, occurs as the reporter protein is secreted by the cells grown in HEK detection. One of the advantages of the secretion of SEAP is the fact that it allows the determination of reporter protein activity without disturbing the cells [56].

SEAP procedure

Before starting the test, it had to be checked that the cells were around 70-80% confluent. After making sure that the cells were at the correct confluency, the positive control Interleukin 1 beta (IL-1β (Sigma. Cat. No. SRP6169)) and the test samples in DPBS (with Ca^{2+}/Mg^{2+}) corresponding to 10x higher than the working concentration were diluted. The samples were diluted 1:10 when adding the cell suspension. To continue, 20 μl of test samples, positive control, and DPBS modified with Ca^{2+}/Mg^{2+}

(as vehicle control) were added per well in the 96-well plate (ThermoFisher. Cat. No 167008) in triplicates. The 96-well plate was then incubated at 37.5 °C for 15 minutes while the cells were being prepared.

A HCT-116-Dual cell (Invivogen, Cat No. hctd-nfis) suspension was prepared by gently rinsing the cells once with DPBS without Ca^{2+}/Mg^{2+}, whereafter the cells were detached by incubating them with 1 ml trypsin at 37.5 °C for 2-3 min. To further ensure the detachment of the cells, the flask containing the cells was tapped. Furthermore, 3 ml DPBS without Ca^{2+}/Mg^{2+} was added and cell clumps dissociated by carefully pipetting up and down. Cells were counted by utilising a hemocytometer and a cell suspension was prepared at $\sim$ 140.000 cells/ml in HEK Detection corresponding to $\sim$ 25.000 cells/well. HEK detection was prepared by dissolving the contents of one pouch of HEK-Blue™ Detection (Invivogen. Cat. No hb-det2) with 50 ml of Ultrapure Water (ThermoFisher. Cat. No. 10977-035). To finalize the procedure, 180 μl of cell suspension ($\sim$ 25.000 cells) were added per well simultaneously with induction using S100A4-Multimer (5 μg/ml (Arxx produced batch)) and IL-1β (0.62-16.6 ng/ml) in three biological replicates and the plate was incubated at 37.5 °C in 5% CO_2 for 24h. S100A4-Multimer and IL-1β were diluted in DPBS with Ca^{2+}/Mg^{2+} (for raw data see appendix 11.2). After incubation at 37.5 °C, the expression of SEAP could be observed with the naked eye and the OD of the samples was measured at a wavelength of 620 nm using a spectrophotometer.

The same procedure was repeated utilising the established polyclonal cell populations from the transfection procedure, the cells coding for RAGE isoform 1 and RAGE isoform 3. Once more, 25.000 cells were seated per well simultaneously with induction using S100A4-Multimer (1.25 μg/ml) and S100A4-Multimer (5 μg/ml), and the positive control of NF-κB, IL-1β (0.62-16.6 ng/ml), to test the responsiveness of the cells to S100A4.

6 Results

Having executed all the needed procedures for the experiment, the following results were obtained and analyzed.

6.1 SEAP assay

Prior to transfection of HCT-116 Dual cells, it is of importance to ensure that cells are not being responsive to S100A4. Hence, the HCT-116 Dual cells were used in the SEAP assay in order to test their responsiveness to S100A4 prior to modifying the cells to express RAGE, by measuring SEAP expression. In addition, this SEAP assay was conducted to investigate the stimulation of NF-κB using IL-1β as a positive control.

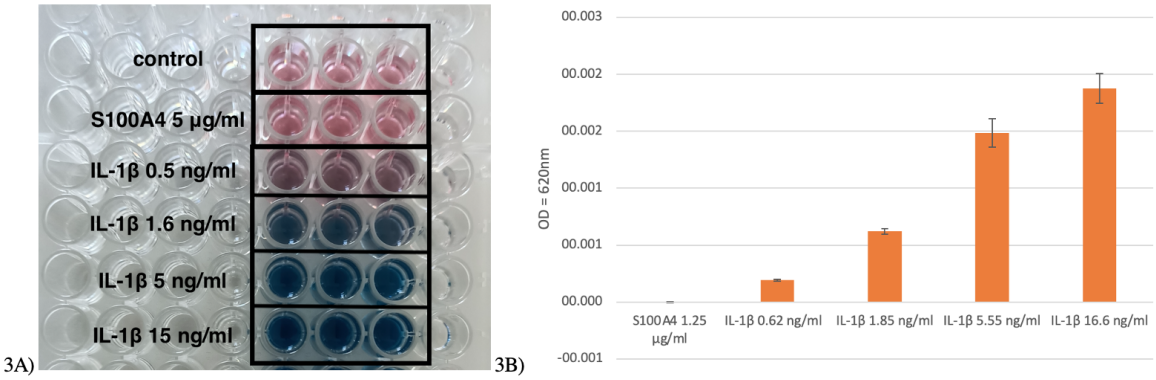

Figure 3: 25.000 cells were seated per well simultaneously with induction using S100A4-Multimer (5 µg/ml) and IL-1β (0.62-16.6 ng/ml) in three biological replicates (for calculations see appendix 11.2). The cells were stimulated 24h, 37.5 °C, 5% CO_2. 3A) A visual impression of the results from the SEAP assay. 3B) A graphical presentation of the result based on absorbance measurements, OD = 620 nm. Error bars indicated standard deviations based on N=3 (for raw data see appendix 11.1).

The results for the SEAP assay of the cells are illustrated in figure 3A. The first three wells are used as blank (vehicle control) for the experiment and contain uninduced cells. As seen with the naked eye, the vehicle control for the experiment resulted in no colour change, confirming that cells that have not been stimulated with a ligand that activates the NF-κB pathway, can not induce the production of SEAP.

The following line of wells accommodate the S100A4 protein. There appeared to be no colour development in the wells, ensuring that the cells do not respond to S100A4.

The following $3 * 4$ wells contained a ranging concentration of the positive control, IL-1β, which is a known initiator of the NF-κB pathway that expresses SEAP if activated. The outcome was that the substrate turned into a purple/blue colour. The colour development of the positive controls ranges alongside the concentration of IL-1β - higher concentration of IL-1β lead to a higher development of colour as a consequence of SEAP hydrolysing the substrate in the HEK detection initiated by IL-1β.

The results gathered in figure 3A were plotted in a bar chart in figure 3B. To plot the results, the absorbance of the solution in the wells was measured at an OD of 620 nm. By making three biological replicates of each solution and calculating the average of these, the likelihood of error is taken into consideration thereby optimizing the results, also known as reproducibility. After calculating the average of the three biological replicates of each solution, the average of the three replicates of vehicle control was subtracted from the induced samples (S100A4-Multimer and IL-1β) to obtain a more precise measurement of absorbance without background noise. Furthermore, the black lines on the bar chart represent the standard deviations calculated from the results of the experiment. The calculated standard deviations describe that the data is not dispersed in relation to the mean to a high degree. Hence, the data is generally clustered around the mean.

The well containing an S100A4 concentration of 5 μg/ml resulted in no absorbance. This further confirms that the cell line does not respond to S100A4 as no colour development was read by measuring the absorbance.

For the remaining four concentrations of the positive control, IL-1β, an increasing absorbance was measured as the concentration of IL-1β increased. Therefore, a higher concentration of IL-1β leads to a higher development of colour.

As a concluding remark, knowing that the cells do not respond to S100A4, the cells are applicable for transfection of RAGE to make the cells responsive to S100A4.

6.2 Transfection of HCT-116 Dual cells

The results gathered in order to establish whether the plasmids had been successfully transfected into the HCT-116 Dual cell line are illustrated in figure 4 and figure 5, respectively.

A transfection mixture was prepared for each plasmid and added to one well of cells:

- One mixture containing the plasmid (M61) coding for RAGE isoform 1 (HCT-116 Dual RAGE 1)
- One mixture containing the plasmid (M83) coding for RAGE isoform 3 (HCT-116 Dual RAGE 3)

In addition, a control was conducted that accommodated cells not being transfected. The purpose of the control is to be a point of comparison for the other tests conducted.

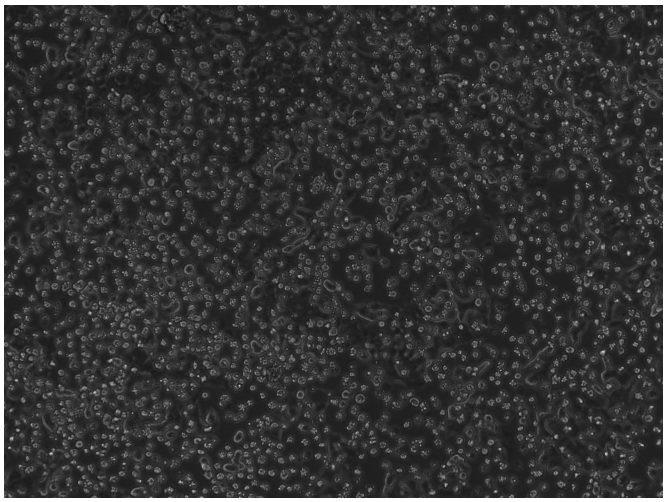

Figure 4: Image taken from the microscope, showing the cells without the expression of the plasmid, no fluorescent colour.

In figure 4, the control containing cells without the expression of RAGE, showed no fluorescent colour when monitored under the fluorescence microscope. This is due to the cells not coding for neither of the plasmids in their genome, moreover not expressing neither of the reporter genes (GFP nor mCherry), which are the two fluorescent proteins that under UV light produce the green and red colour. Hence, these reporter genes are visual indicators of successful transfection.

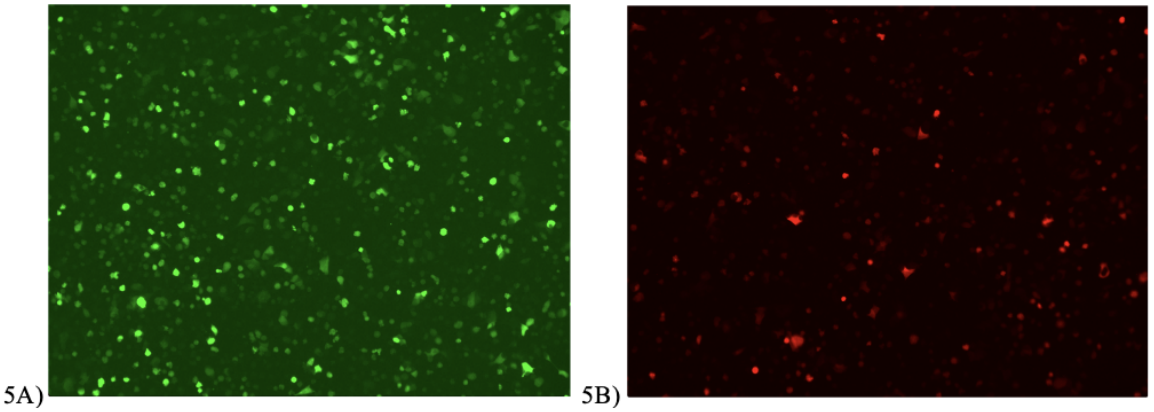

Figure 5: Fluorescence microscope images illustrating HCT-116 Dual RAGE 1 as illustrated on figure 5A, and HCT-116 Dual RAGE 3 as demonstrated on figure 5B.

Figure 5 demonstrates that the cells exhibit green fluorescence when monitored under the fluorescence microscope, a day post transfection of the cells. Therefore, the cells have effectively been transformed with the GFP-tagged plasmid coding for RAGE-isoform 1. It also shows the fluorescent red colour of the cells under the fluorescence microscope, indicating that the cells express the mCherry-tagged plasmid coding for RAGE-isoform 3.

6.3 Selection of HCT-116 Dual RAGE clones

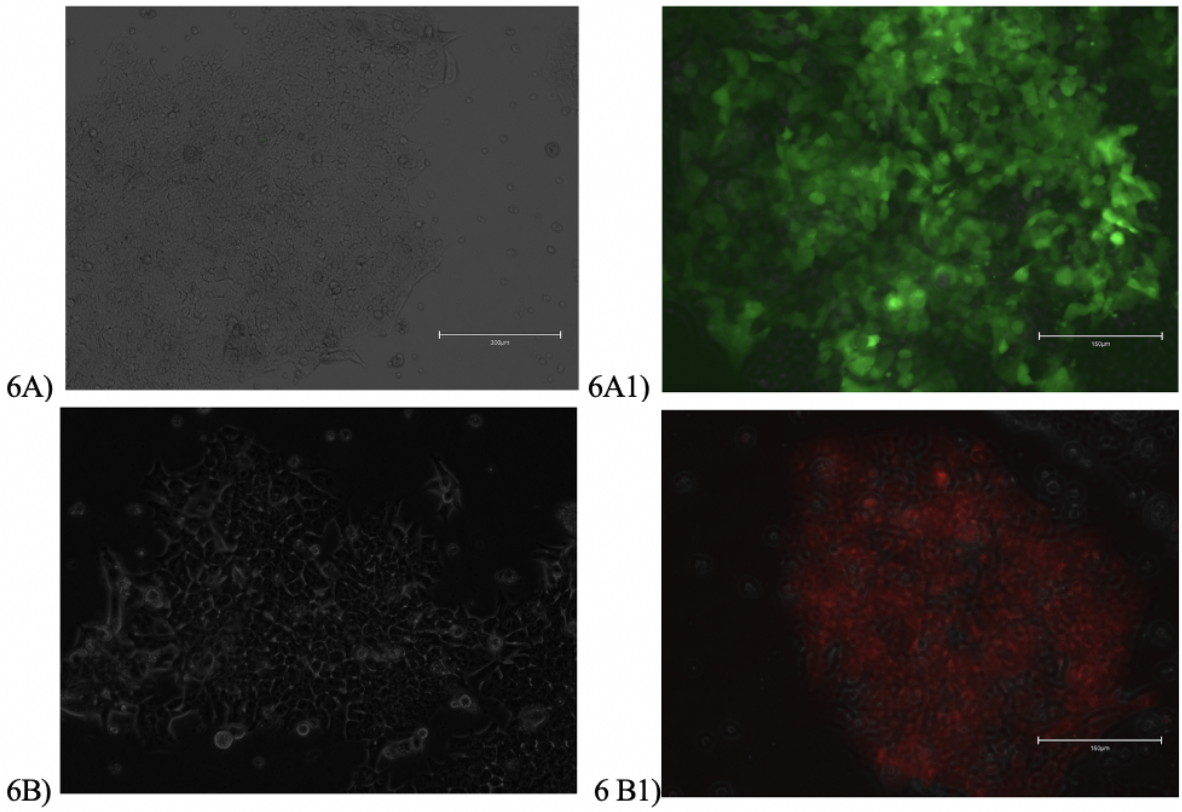

Figure 6: Figure 6A and 6A1 illustrate HCT-116 Dual RAGE 1. Figure 6A depicts the transfected cells as captured by a light microscope, and figure 6A1 illustrates the same cells when monitored under a fluorescence microscope. Figure 6B and 6B1 illustrate HCT-116 Dual RAGE 3. Figure 6B depicts the transfected cells as captured by a light microscope, and figure 6B1 illustrates the same cells when monitored under a fluorescence microscope.

As suspected, the results gathered from the transfection illustrated in figure 6, after the addition of selective antibiotics [1 mg/ml G418 (neomycin)] to the pool of cells, all cells not expressing the NeoR/KanR antibiotic resistant gene in their genome died, and only living cells adhered to the plate.

Figure 6A1 and 6B1 indicate different levels of fluorescence in the cells; some showing high fluorescence and others barely showing any. Since most of the clones appear fluorescent, high transfection efficacy can be concluded.

The transfection procedure was successful and two polyclonal cell populations were established:

- HCT-116 Dual RAGE 1
- HCT-116 Dual RAGE 3

This was done by pooling several clones in cell culture flasks until an efficient amount of cells expressing the plasmids were obtained prior to initiating the SEAP assay.

6.4 The ability of S100A4 to stimulate HCT-116 Dual RAGE 1 and HCT-116 Dual RAGE 3

The expected outcome for the SEAP experiment was the binding of S100A4 to RAGE isoform 1 that initiates MAPK (ERK) phosphorylation, activating NF-κB, which then enters the nucleus of the cell, initiating gene expression. SEAP is an enzyme that specifically expresses if a ligand initiates the NF-κB pathway, which S100A4 supposedly does when binding to RAGE isoform 1. SEAP is measured by seeding cells in HEK detection, having a substrate that SEAP converts to express a purple/blue colour, allowing for colourimetric measurement.

HCT-116 Dual RAGE 1 and HCT-116 Dual RAGE 3 were stimulated with S100A4 and the positive control of NF-κB, IL-1β, to test the responsiveness of the cells to S100A4. It was hypothesized that S100A4 would be able to bind to HCT-116 Dual RAGE 1, but not to HCT-116 Dual RAGE 3. Thus, SEAP activity would thereby be expressed by purple/blue colour formation as a result of S100A4 interacting with RAGE isoform 1 and not for the interaction between S100A4 and RAGE isoform 3. The results showed that neither cells coding for RAGE isoform 1 nor the cells coding for RAGE isoform 3 responded to S100A4.

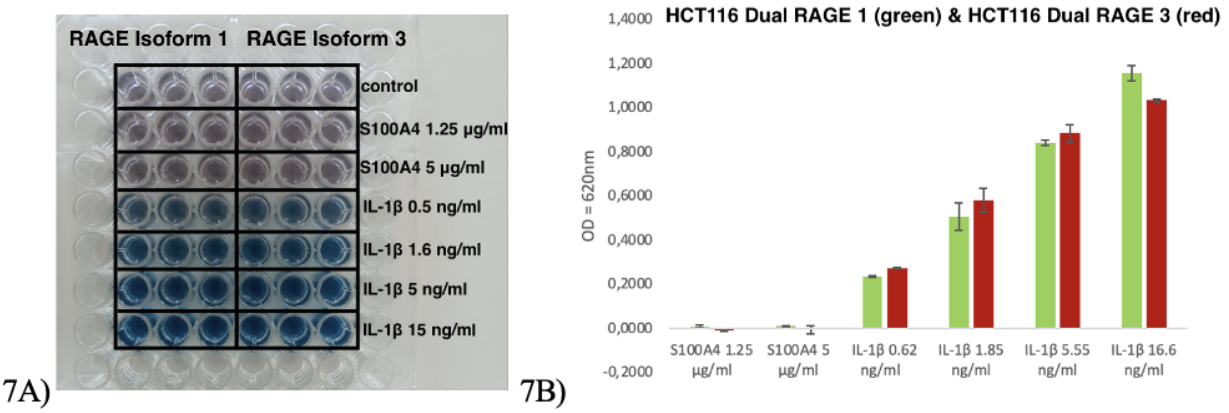

Figure 7: 25.000 cells were seated per well simultaneously with induction using S100A4-Multimer (1.25 µg/ml) and S100A4-Multimer (5 µg/ml), and IL-1β (0.62-16.6 ng/ml) in three biological replicates (for calculations see appendix 11.2) The cells were stimulated 24 h, 37.5 °C, 5% CO2. 7A) A visual impression of the results from the SEAP assay, where HCT-116 Dual RAGE 1 and HCT-116 Dual RAGE 3 created during transfection were utilised. 7B) A graphical representation of the results based on absorbance measurements, OD = 620 nm. Error bars indicated standard deviations based on N=3 (for raw data see appendix 11.3).

The results are illustrated in figure 7. As seen in figure 7A, the first line horizontally is used as blank (vehicle control) for the experiment, which resulted in no colour

change. The following two lines accommodated the S100A4 protein in two different concentrations (1.25 μg/ml and 5 μg/ml). There appeared to be no colour development in the wells, assuring that the cells were unresponsive to stimulation with S100A4. The following wells contained a ranging concentration of IL-1β, with an outcome represented by the substrate in HEK detection turning into a purple/blue colour when initiated by the positive control. Figure 7B, represents the results from figure 7A plotted in a bar chart.

As previously conducted, the absorbance of the solution in the wells was measured with a spectrophotometer at an OD of 620 nm, the wavelength of blue colour. After calculating the average of the three biological replicates of vehicle control, it was subtracted from the induced samples (S100A4 and IL-1β) to obtain a more precise measurement of absorbance without background noise. The standard deviations are represented by the black lines on the bar chart. It can be seen that the level of absorbance monitored does not differ substantially between the HCT-116 Dual RAGE 1 and HCT-116 Dual RAGE 3 for both the induction with S100A4-Multimer and IL-1β.

Contrary to what was expected, SEAP is not expressed when induced by S100A4 for both HCT-116 Dual RAGE 1 and HCT-116 Dual RAGE 3, indicated by no purple/blue colour formation present in the cell wells.

7 Discussion

In the following section, the results gathered in the experiment will be discussed to determine whether the set hypothesis will be confirmed or rejected.

Due to time restrictions, the procedure of this study was only conducted once. For proper examination of results, it is of importance to conduct multiple trials of the experiment to verify that the results obtained are adequate. Therefore, the discussion is based on the assumption that the results gathered are valid, however, they should be considered preliminary.

After transfection, the addition of the medium containing selective antibiotics [1 mg/ml G418 (neomycin)] to the cells was not as effective as expected. The cells clustered, making them less sensitive to selective antibiotics. This overgrowth is related to the high proliferation rate of the HCT-116 Dual cell line as well as the addition of too many cells to the 10 cm culture dish. Thus, the cells were trypsinized in order to reduce the number of cells and spread them out. This made the selection with G418 more effective. After the transfection, the established biological clones were pooled together to obtain polyclonal populations with HCT-116 Dual RAGE 1 and HCT-116 Dual RAGE 3, respectively, because the high proliferation rates made it difficult to separate some clones and, by pooling, it was possible to initiate the SEAP assay earlier.

Due to time restrictions, it was chosen to perform this project on polyclonal populations, thereby skipping population selection to generate a monoclonal population, as they take longer to create. The polyclonal population was thereby both containing the successfully transfected as well as the non-transfected cells, potentially weakening our analysis. Furthermore, for the HCT-116 cell-based model system, it could have been beneficial to have utilised a monoclonal population, as it allows for easier selection of the best clones for this setup in terms of RAGE expression levels and SEAP expression. This is because monoclonal populations are more homogeneous since they come from one single cell. On the contrary, a polyclonal population is more heterogeneous and can cause variability over time. It is therefore not possible to check where the plasmid is integrated into the genome in polyclonal populations, but by adding antibiotics to the growth medium, the growth of the cells expressing the plasmids is favoured. Nevertheless, there are also advantages to having a polyclonal population, as their heterogeneous traits allow them to mimic the nature of naturally occurring heterogeneous populations. For future experiments, fewer cells could have been added to the 10 cm culture dish, in order to achieve a better separation of the cells, thus, assuring that the cells become less clustered, prior to selecting them. In this study, 1:2 of the transfected cells were utilised in the SEAP assay. If repeated, an idea could have been to add 1:10 of the transfected

cells instead to assure a higher spread of clones within the culture dish, allowing for easier selection of populations.

As seen in the results for the SEAP experiment illustrated in figure 7, SEAP was not expressed when stimulated by S100A4 for both the polyclonal cell populations established, HCT-116 Dual RAGE 1 and HCT-116 Dual RAGE 3. Even though the results portray that S100A4 is not able to induce SEAP in the cells when binding to RAGE, there are multiple factors that could have affected the cells to be unresponsive to S100A4 in this particular experiment. Accordingly, there are many steps that must be ensured in order for RAGE to become properly expressed by the cells, including three of great importance:

- The first is a successful transcription of the gene coding for RAGE when the plasmids were inserted into the HCT-116 Dual cell line by transfection. Solution - Real-time quantitative polymerase chain reaction (qPCR).
- The second is that RAGE may not have been translated into a protein. Solution - Western blot.
- The last step is that RAGE might not have arrived at its final placement in the cell membrane, where it acts as a receptor. Solution - Immunofluorescence staining.

All the above parameters need to be investigated prior to drawing any concluding remarks in regards to answering the *'why'* behind the cells being unresponsive to S100A4 - differing from the theoretical evidence of S100A4 interacting with RAGE as experimentally proven in the study by M. Dahlmann, et. al., 2014 [43], which was the key motivational paper for this study.

The journey from gene to protein is complex and tightly controlled within each cell and differs between cell types, consisting of two major steps known as transcription and translation, all summarised by the central dogma in molecular biology. Hence, errors in information transfer from DNA to RNA to protein are inevitable [44].

Despite the fact that fluorescence clones were created, indicating successful transfection as seen in figure 6, it does not provide proof that RAGE has been effectively expressed as a functioning receptor. The results only enable us to validate that the cells have been transformed with this newly created GFP- or mCherry-tagged DNA, and that in theory because the plasmids both contain a site for the GOI (RAGE) and a site for the reporter gene (either GFP or mCherry), they will be transcribed together. However, a wide range of transcription based errors could have arisen during the transcription of the gene coding for RAGE, directly producing mRNA transcripts differing from the DNA template [48]. Most errors occurring during transcription are caused by mispairings

of nucleotides, known as small-scale mutations that involve the change in one DNA nucleoside pair. These small-scale mutations are further classified into substitution mutations, insertions, and deletions. Nucleoside-pair substitutions can cause missense and nonsense mutations. Missense mutations change an amino acid to another amino acid. Nonsense mutations change an amino acid to a STOP codon, resulting in premature termination of translation [48]. Replication errors can also involve insertions or deletions of nucleotide bases that occur during a process called strand slippage [62]. These nucleotide-pair insertions or deletions may produce frameshift mutations, which usually introduce premature STOP codons in addition to lots of amino acid changes [48]. Additionally, epigenetic mutations are another error that could have arisen during the transcription of the gene coding for RAGE. Epigenetic mutations can be described as a heritable change in gene expression that does not affect the actual base-pair sequence of DNA, but that constitute clonally heritable alterations in the transcriptional status of a gene that leads to the abnormal silencing of that gene [45]. Additionally, mutations outside the coding sequence could also have impacted gene expression.

Further research could have been done to test whether the GOI had been expressed, and to what extent, by using real-time qPCR. After the transfection step, where two new cell lines were created, HCT-116 Dual RAGE 1 and HCT-116 Dual RAGE 3, qPCR can be used to investigate whether RAGE is expressed to a higher degree than in the untransfected HCT-116 Dual cells. This is done by isolating RNA from the cells, representing the transcriptome, and investigating the level of RNA generated that match the RAGE transcript. The RNA is converted to complementary DNA (cDNA) and via primers specific for RAGE amplified via real-time qPCR giving an intensity read corresponding to the level of expression. Hence, the test allows measuring if the gene coding for RAGE has been properly transcribed into mRNA [66, 67].

Translation is highly prone to error, providing the high likelihood of RAGE not being efficiently translated into a protein. Erroneous protein synthesis is defined as any disruption found in the conversion of a coding sequence into a functioning protein. Amino-acid misincorporations are the most common error during translation. Amino-acid misincorporations are inherent and unintended errant replacements of amino acids. Accordingly, polypeptide errors can induce protein misfolding, aggregation, and cell death. The generation of a functional protein can as well already be affected by the transcript in form of a wide range of mutations under transcription. This can lead to aberrant splicing, premature termination, faulty post-translational modifications, and kinetic missteps during folding. Additionally, correctly synthesized proteins can also fail to fold into a functional protein [46].

In order to have further ensured that the gene coding for RAGE had completed

translation into protein, the technique, western blotting, could have been utilised. The technique allows researchers to identify specific proteins from complex mixtures of proteins extracted from cells. Western blotting is a protein staining method. The method consists of three parts: separating target proteins by size (gel electrophoresis), transferring them to a solid support, and marking target proteins with the appropriate primary and secondary antibodies for visualization (immunostaining procedure) [47]. The technique is done by loading the protein of interest (RAGE) into a gel consisting of a positive and negative pole. Since proteins are negatively charged, they are drawn to the positive pole. The gel allows migration based on size, thus the larger proteins will migrate a shorter distance in comparison to the shorter proteins. Western blotting can both be made with proteins in their 3D structure as well as proteins in their amino acid chain (2D), both of which are relevant depending on what is being examined. The 3D structure of the receptor is of great importance as it provides knowledge in regards to understanding how the protein functions, including predicting what ligands bind to that protein, thereby gaining a better understanding of what biological interactions can occur, moreover what transmembrane signal transduction can take place. For instance, if western blotting had been conducted on the 3D structure of the protein, RAGE, and the protein had migrated further than theoretically established, then it would indicate that the folding of the receptor had gone wrong. However, if the 2D structure of RAGE was examined, it would be plausible to distinguish between different isoforms of the particular protein. Thus, the 2D structure allows the detection of any errors that might occur during the translation of RAGE into protein, for instance, if premature termination or faulty posttranslational modifications have taken place [64, 65].

Even if RAGE is properly translated, the protein must be correctly located in the cell membrane. If RAGE has not been properly expressed in the cell membrane, the lack of binding site for extracellular S100A4 could lead to the results showing no expression of SEAP. Even though the gene coding for RAGE could have been successfully transcribed and translated, there are multiple steps the protein encounters before arriving at the destination of its function, described as the journey of a protein through the endomembrane system. When a protein has been synthesized in the cytoplasm by the ribosomes, they travel to the rough endoplasmic reticulum (ER), where they undergo modifications. These modified proteins may be absorbed into the membrane of the ER or packaged into a vesicle that travels to the Golgi apparatus. At the Golgi apparatus, the proteins encounter further modifications and are sorted, packaged, and tagged, so they can travel through vesicles to their target destination of function, inside or outside of the cell [60]. Therefore the protein coding for RAGE could have been tagged wrongly during the protein synthesis, and not arrived at its final destination in the cell membrane, where it acts as a receptor; consequently, leading to S100A4 not being able to induce SEAP. Accordingly, in the course of the journey of the protein through the

endomembrane system, where the protein undergoes post-translational modifications, errors during modification could have arisen, thereby affecting the expression of RAGE.

To validate RAGE location, immunofluorescence staining could have been utilised to assess the location and expression of RAGE within the cells. The principle of immunofluorescence assays is based on two steps: the first being that specific primary antibodies bind to the protein of interest (RAGE) and the second being that secondary fluorophore-coupled antibodies bind to the primary antibodies, thereby visualizing the protein of interest (RAGE) by microscopy. Accordingly, it is possible to detect where and if RAGE is expressed and located in the cell, intracellularly, or on the cell surface [61].

A significant limitation to the study was time. In order to have done proper experimental research, each of the variables in the procedure should have been isolated and tested to ensure higher accuracy. As mentioned prior, in this study the tests that could have allowed for higher precision in the results are western blotting and qPCR, respectively. Additionally, an experimental error is always possible. Any time a qualitative or quantitative observation has been made, there is a degree of uncertainty. This can be due to a range of preexisting limitations such as inaccuracies in apparatus used or inaccuracies in measuring techniques done, e.g. pipetting errors. Proper use of a pipette requires precision, not only when setting the quantity of liquid to be aspirated, but also when using the pipette itself, ensuring the right angle, applying the right pressure, and releasing the pressure correctly after use.

Moreover, the topic of this project was something completely new for the group. Therefore, it was challenging to start at the beginning, as a lot of research and understanding of the background theory on an academic level was acquired. This process required time and effort that could instead be put into conducting more steps in the experimental procedure, which could have allowed for greater certainty of the reason behind S100A4 being unresponsive.

8 Conclusion

In order to conclude on the gathered outcomes, every aspect of the results must be taken into consideration. In regards to the SEAP assay, the experiment confirmed that SEAP is expressed when induced with IL-1β, providing the information that SEAP can be expressed if induced with a ligand that stimulates the activation of the transcription factor, NF-κB. Furthermore, the results confirmed that the parental HCT-116 Dual cell line did not respond to S100A4 prior to the creation of the clones during the transfection. Additionally, polyclonal cell populations were successfully obtained, here HCT-116 Dual RAGE 1 and HCT-116 Dual RAGE 3, respectively, as indicated by most clones appearing to be fluorescent, thus high transfection efficacy could be affirmed.

It was initially hypothesized that S100A4 would bind to HCT-116 Dual RAGE 1 and not HCT-116 Dual RAGE 3 as evidence indicates that S100A4 binds to the hydrophobic region on the V1 domain of RAGE isoform 1. Based on this study, no concluding remarks can be made on whether or not S100A4 only binds to RAGE isoform 1 and not isoform 3 as the cells were not responsive to S100A4 post transfection in either clone. The present results contradict previous findings, therefore, many validation steps and optimizations of the protocol are needed for future experiments. Even though the results portray that S100A4 is not able to induce SEAP in the cells when binding to RAGE, there are multiple factors that could have affected the cells to become unresponsive to S100A4 for this particular experiment. For future experimental work, the set procedure thereby needs to be repeated, wherein a monoclonal selection step could be highly beneficial. Additionally, the RAGE transcription, translation, binding affinity, and location need to be validated. This could be done by utilising a variety of methods that focus on examining RAGE expression and the overall S100A4-RAGE-interaction.

9 Perspective

This paper was conducted with the aim of focusing on the interaction site by which S100A4 binds to RAGE, within fibrosis in SSc. However, this interaction should evidently be similar in most fibrotic diseases, multifarious fibrotic diseases could thereby have been researched. The reason why SSc was the chosen disease in this project was due to SSc being a 'prototypic´ fibrotic disease. This means that SSc is a disease that follows the typical nosogenesis expected for a fibrotic disease. As SSc acts as a "model" fibrotic disease, research done on SSc can be applied to most other fibrotic diseases.

Had there been more time available, an examination of which cell lines are better for investigating the interaction between S100A4 and RAGE could have been conducted. This could have potentially led to an optimization of the results gathered in vitro. This examination is presented in a study published by M. Dahlmann, et. al., 2014 [43].

Another angle to the study could have been to further examine the S100A4-RAGE-interaction. An experiment upon the influence of the S100A4 and RAGE interaction on motility and invasion could have been conducted. This would be done through a scratch assay. During a scratch assay (wound-healing assay), cells are grown in a monolayer, whereafter a scratch is made with a pipette tip to create a gap corresponding to a "wound". The "wounded" area is then photographed to determine the cell migration rate. The percentage of closure of the scratch area is then calculated [50]. Through this technique, it would have been possible to determine the more specific impacts of S100A4-RAGE-interaction on wound healing and, moreover, healing within fibrotic tissue.

Additionally, an experiment could have been conducted to examine the impacts of blocking the expression of S100A4 or RAGE in fibrotic tissue. According to the study made by Herwig N. et. al., 2016, an experiment on the blocking of S100A4 secretion was conducted [15]. The blocking of S100A4 secretion was done through secretion of Brefeldin A (BFA), gene silencing by short interfering RNA (siRNA), or addition of either recombinant S100A4 or sRAGE. This is done in order to examine the prometastatic effects of S100A4. It was seen that the blockage of S100A4 led to a decrease in cell motility. Furthermore, the addition of S100A4 to the tested cells leads to an increase in the cell migratory behavior. This experiment was, however, not conducted on fibrotic cells, it would thereby have been interesting to examine the mechanism in fibrotic tissue, as well as the impacts on gene expression.

An alternative approach to the current study could have been to consider new therapeutic strategies for SSc, as no known cure for this disease has been found. Current

treatment is exclusively focused on relieving symptoms or preventing the disease from further progressing. Additionally, a high level of S100A4 in the serum of patients with fibrotic diseases closely correlates with disease activity, serving as a biomarker for early diagnosis and surveillance [9]. Hence, patients with SSc have an upregulation of the S100A4 protein in their skin [26]. A study of knockout mouse models suggests that extracellular S100A4 may function as a therapeutic target for fibrotic diseases if suppressing expression, release, or function can be achieved [9]. This suggests that inhibiting the protein's expression, release or function might be a promising therapeutic strategy. In addition, in a study done on patients with SSc, the receptor RAGE was found in skin biopsies of the patients [13]. Understanding the key pathogenetic pathways involved in disease expression allows for the development of targeted therapies. Furthermore, indicating that the knockout of S100A4 or RAGE could be a way of creating a new therapeutic target for fibrotic diseases.

In order to block the expression of S100A4 or RAGE, a closer look upon regulation of gene expression would be needed. miRNA or siRNA can block translational mRNAs. MicroRNAs (miRNAs) are small ssRNA molecules that can bind to mRNA. They're formed by the processing of a longer precursor. siRNA or miRNA forms a complex with proteins that can degrade mRNA or block its translation [48]. In this way knockout of the two GOI could be a strategy to inhibit either the protein or the receptor's expression, release, or function.

10 References

[1] Allanore, Y., Simms, R., Distler, O., et. al. (2015). "Systemic Sclerosis". *Nature reviews. Disease primers, 1*, 15002. https://doi.org/10.1038/nrdp.2015.2. PMID: 27189141

[2] Healthline, Author: Herndon, J., et. al. (2022). *Systemic Sclerosis (Scleroderma).* URL: https://www.healthline.com/health/scleroderma. (Last updated: 7.03.2022). (Accessed: 17.05.2022).

[3] Mayo clinic. (2022). *Scleroderma.* URL: https://www.mayoclinic.org/diseases-conditions/scleroderma/symptoms-causes/syc-20351952. (Accessed: 17.05.2022).

[4] Sierra-Sepúlveda, A., Esquinca-González, A., Benavides-Suárez, S. A., et. al. (2019). "Systemic Sclerosis Pathogenesis and Emerging Therapies, beyond the Fibroblast". *BioMed research international*, 2019, 4569826. https://doi.org/10.1155/2019/4569826. PMID: 30809542. PMCID: PMC6364098.

[5] Wynn T. A. (2008). "Cellular and molecular mechanisms of fibrosis". *The Journal of pathology, 214* (2), 199–210. https://doi.org/10.1002/path.2277.PMID: 18161745. PMCID: PMC2693329.

[6] Wynn, T. A., Ramalingam, T. R. (2012). "Mechanisms of fibrosis: therapeutic translation for fibrotic disease". *Nature medicine*, 18(7), 1028–1040. https://doi.org/10.1038/nm.2807. PMID: 22772564. PMCID: PMC3405917.

[7] Baraut, J., Michel, L., Verrecchia, F., et. al. (2010). "Relationship between cytokine profiles and clinical outcomes in patients with systemic sclerosis". *Autoimmunity reviews, 10* (2), 65–73. https://doi.org/10.1016/j.autrev.2010.08.003. PMID: 20713187.

[8] PROSPEC Protein Specialists. *Growth factors.* URL: https://www.prospecbio.com/growth_factors. (Accessed: 17.05.2022).

[9] Li, Z., Li, Y., Liu, S., et. al. (2020). "Extracellular S100A4 as a key player in fibrotic diseases". *Journal of cellular and molecular medicine, 24*, (11), 5973–5983. https://doi.org/10.1111/jcmm.15259. PMID: 32307910. PMCID: PMC7294136.

[10] Roh, J. S., Sohn, D. H. (2018). "Damage-Associated Molecular Patterns in Inflammatory Diseases". *Immune network, 18* (4), e27. https://doi.org/10.4110/in.2018.18.e27. PMID: 30181915. PMCID: PMC6117512.

[11] Sparvero, L.J., Asafu-Adjei, D., Kang, R. et al. "RAGE (Receptor for Advanced Glycation Endproducts), RAGE Ligands, and their role in Cancer and Inflammation". *Journal of translational medicine, 7*, 17. https://doi.org/10.1186/1479-5876-7-17. PMID: 19292913. PMCID: PMC2666642.

[12] van Zoelen, M. A., Achouiti, A., van der Poll, T. (2011). "The role of receptor for advanced glycation endproducts (RAGE) in infection". *Critical care (London, England), 15*(2), 208. https://doi.org/10.1186/cc9990. PMID: 21457506. PMCID: PMC3219404.

[13] Davies, C. A., Herrick, A. L., Cordingley, L., et. al. (2009). "Expression of advanced glycation end products and their receptor in skin from patients with systemic sclerosis with and without calcinosis". *Rheumatology (Oxford, England), 48*(8), 876–882. https://doi.org/10.1093/rheumatology/kep151 PMID: 19542215.

[14] Ding, Q., Keller, J. N. (2005). "Evaluation of rage isoforms, ligands, and signaling in the brain". *Biochimica et biophysica acta, 1746*(1), 18–27. https://doi.org/10.1016/j.bbamcr.2005.08.006. PMID: 16214242.

[15] Herwig, N., Belter, B., Wolf, S., et. al. (2016). "Interaction of extracellular S100A4 with RAGE prompts prometastatic activation of A375 melanoma cells". *Journal of cellular and molecular medicine, 20*(5), 825–835. https://doi.org/10.1111/jcmm.12808. PMID: 26928771. PMCID: PMC4831350.

[16] Bhattacharyya, S., Wei, J., Varga, J. (2011). "Understanding fibrosis in systemic sclerosis: shifting paradigms, emerging opportunities". *Nature reviews. Rheumatology, 8*(1), 42–54. https://doi.org/10.1038/nrrheum.2011.149. PMID: 22025123. PMCID: PMC3954787.

[17] Weiskirchen, R., Weiskirchen, S., Tacke, F. (2019). "Organ and tissue fibrosis: Molecular signals, cellular mechanisms and translational implications". *Molecular aspects of medicine, 65*, 2–15. https://doi.org/10.1016/j.mam.2018.06.003. PMID: 29958900.

[18] Zhang, W. J., Chen, S. J., Zhou, S. C., et. al. (2021). "Inflammasomes and Fibrosis". *Frontiers in immunology, 12*, 643149. https://doi.org/10.3389/fimmu.2021.643149. PMID: 34177893. PMCID: PMC8226128.

[19] Wynn T. A. (2008). "Cellular and molecular mechanisms of fibrosis". *The Journal of pathology, 214*(2), 199–210. https://doi.org/10.1002/path.2277. PMID: 18161745. PMCID: PMC2693329.

[20] Baum, J., Duffy, H. S. (2011). "Fibroblasts and myofibroblasts: what are we talking about?". *Journal of cardiovascular pharmacology, 57*(4), 376–379. https://doi.org/10.1097/FJC.0b013e3182116e39. PMID: 21297493. PMCID: PMC3077448.

[21] Kendall, R. T., Feghali-Bostwick, C. A. (2014). "Fibroblasts in fibrosis: novel roles and mediators". *Frontiers in pharmacology, 5,* 123. https://doi.org/10.3389/fphar.2014.00123. PMID: 24904424. PMCID: PMC4034148.

[22] Wyczanska, M., Lange-Sperandio, B. (2020). "DAMPs in Unilateral Ureteral Obstruction". *Frontiers in immunology, 11*, 581300. https://doi.org/10.3389/fimmu.2020.581300. PMID: 33117389. PMCID: PMC7575708.

[23] Bagalad, B. S., Mohan Kumar, K. P., Puneeth, H. K. (2017). "Myofibroblasts: Master of disguise". *Journal of oral and maxillofacial pathology : JOMFP, 21*(3), 462–463. https://doi.org/10.4103/jomfp.JOMFP_146_15. PMID: 29391737. PMCID: PMC5763885.

[24] van Beurden, H. E., Von den Hoff, J. W., Torensma, R., et. al. (2005). "Myofibroblasts in palatal wound healing: prospects for the reduction of wound contraction after cleft palate repair". *Journal of dental research, 84*(10), 871–880. https://doi.org/10.1177/154405910508401002. PMID: 16183784.

[25] Yue B. (2014). "Biology of the extracellular matrix: an overview". *Journal of glaucoma, 23*(8 Suppl 1), S20–S23. https://doi.org/10.1097/IJG.0000000000000108. PMID: 25275899. PMCID: PMC4185430.

[26] Ambartsumian, N., Klingelhöfer, J., Grigorian, M. (2019). "The Multifaceted S100A4 Protein in Cancer and Inflammation". *Methods in molecular biology (Clifton, N.J.), 1929*, 339–365. https://doi.org/10.1007/978-1-4939-9030-6_22. PMID: 30710284.

[27] Bard, J. (2008). "Morphogenesis". *Scholarpedia 3*(6), 2422. doi:10.4249/scholarpedia.2422. URL: http://www.scholarpedia.org/article/Morphogenesis.

[28] Leclerc, E., Fritz, G., Vetter, S. W., et. al. (2009). "Binding of S100 proteins to RAGE: an update". *Biochimica et biophysica acta, 1793*(6), 993–1007. https://doi.org/10.1016/j.bbamcr.2008.11.016. PMID: 19121341.

[29] Walsh, D. A., Pearson, C. I. (2001). "Angiogenesis in the pathogenesis of inflammatory joint and lung diseases". *Arthritis research, 3*(3), 147–153.

https://doi.org/10.1186/ar292. PMID: 11299055. PMCID: PMC128891.

[30] McCain J. (2013). "The MAPK (ERK) Pathway: Investigational Combinations for the Treatment Of BRAF-Mutated Metastatic Melanoma". *P T : a peer-reviewed journal for formulary management, 38*(2), 96–108. PMID: 23599677. PMCID: PMC3628180.

[31] Liu, T., Zhang, L., Joo, D., et. al. (2017). "NF-B signaling in inflammation". *Signal transduction and targeted therapy, 2,* 17023–. https://doi.org/10.1038/sigtrans.2017.23. PMID: 29158945. PMCID: PMC5661633.

[32] Dong, J., Ma, Q. (2019). "In Vivo Activation and Pro-Fibrotic Function of NF-κB in Fibroblastic Cells During Pulmonary Inflammation and Fibrosis Induced by Carbon Nanotubes". *Frontiers in pharmacology, 10*, 1140. https://doi.org/10.3389/fphar.2019.01140. PMID: 31632276. PMCID: PMC6783511.

[33] Dolcet, X., Llobet, D., Pallares, J., et. al. (2005). "NF-kB in development and progression of human cancer". *Virchows Archiv : an international journal of pathology, 446*(5), 475–482. https://doi.org/10.1007/s00428-005-1264-9. PMID: 15856292

[34] Biology Online. *Cell line.* URL: https://www.biologyonline.com/dictionary/cell-line. (Last updated: 24.02.2022) (Accesssed: 17.05.2022).

[35] Kaur, G., Dufour, J. M. (2012). "Cell lines: Valuable tools or useless artifacts". *Spermatogenesis, 2*(1), 1–5. https://doi.org/10.4161/spmg.19885. PMID: 22553484. PMCID: PMC3341241.

[36] TermoFisher Scientific. *Introduction to Transfection* URL: https://www.thermofisher.com/dk/en/home/references/gibco-cell-culture-basics/transfection-basics/introduction-to-transfection.html. (Accessed: 17.05.2022).

[37] Sheikh, S., Coutts, A. S., La Thangue, N. B. "Transfection". (2017). In: *Basic Science Methods for Clinical Researchers*, pp. 191-209. https://doi.org/10.1016/B978-0-12-803077-6.00011-4.

[38] TermoFisher Scientific. *Reporter Gene Assays.* URL: https://www.thermofisher.com/dk/en/home/references/gibco-cell-culture-basics/transfection-basics/reporter-gene-assays.html. (Accessed: 17.05.2022).

[39] Tannous, B. A., Teng, J. (2011). "Secreted blood reporters: insights and applications". *Biotechnology advances, 29*(6), 997–1003. https://doi.org/10.1016/j.biotechadv.2011.08.021. PMID: 21920429. PMCID:

PMC3189544.

[40] Ding, Q., Keller, J. N. (2005). "Evaluation of rage isoforms, ligands, and signaling in the brain". *Biochimica et biophysica acta, 1746*(1), 18–27. https://doi.org/10.1016/j.bbamcr.2005.08.006. PMID: 16214242.

[41] Juranek, Judyta Banach, Marta. (2015). "The role of RAGE in the diabetic neuropathy (Rola białka RAGE w neuropatii cukrzycowej)". *Family Medicine and Primary Care Review. 2015; 17,*4: 316–318. doi: 10.5114/fmpcr/60316.

[42] Muthyalaiah, Y. S., Jonnalagadda, B., John, C. M., et. al. (2021). "Impact of Advanced Glycation End products (AGEs) and its receptor (RAGE) on cancer metabolic signaling pathways and its progression". *Glycoconjugate journal, 38*(6), 717–734. https://doi.org/10.1007/s10719-021-10031-x. PMID: 35064413.

[43] Dahlmann, M., Okhrimenko, A., Marcinkowski, P., Osterland, M., et. al. (2014). "RAGE mediates S100A4-induced cell motility via MAPK/ERK and hypoxia signaling and is a prognostic biomarker for human colorectal cancer metastasis". *Oncotarget, 5*(10), 3220–3233. https://doi.org/10.18632/oncotarget.1908. PMID: 24952599. PMCID: PMC4102805.

[44] Gordon, A. J., Satory, D., Halliday, J. A., et. al. (2015). "Lost in transcription: transient errors in information transfer". *Current opinion in microbiology, 24*, 80–87. https://doi.org/10.1016/j.mib.2015.01.010. PMID: 25637723. PMCID: PMC4380820.

[45] Antonarakis, S. E., Cooper, D. N. (2019) "Human Genomic Variants and Inherited Disease: Molecular Mechanisms and Clinical Consequences" *Emery and Rimoin's Principles and Practice of Medical Genetics and Genomics (Seventh Edition)*. pp. 125-200. https://doi.org/10.1016/B978-0-12-812537-3.00006-8.

[46] Drummond, D. A., Wilke, C. O. (2009). "The evolutionary consequences of erroneous protein synthesis". *Nature reviews. Genetics, 10*(10), 715–724. https://doi.org/10.1038/nrg2662. PMID: 19763154. PMCID: PMC2764353.

[47] Mahmood, T., Yang, P. C. (2012). "Western blot: technique, theory, and trouble shooting". *North American journal of medical sciences, 4*(9), 429–434. https://doi.org/10.4103/1947-2714.100998. PMID: 23050259. PMCID: PMC3456489.

[48] Urry, L. A., Cain, M. L., Wasserman, P. V., et. al. (2021). "CAMPBELL BIOLOGY". Description: Twelfth edition. *New York, NY : Pearson, 2020.*

[49] Altschuler, S. J., Wu, L. F. (2010). "Cellular heterogeneity: do differences make a

difference?". *Cell, 141*(4), 559–563. https://doi.org/10.1016/j.cell.2010.04.033. PMID: 20478246. PMCID: PMC2918286.

[50] Gordillo, G. M., Bernatchez, S. F., Diegelmann, R., et. al. (2013). "Preclinical Models of Wound Healing: Is Man the Model? Proceedings of the Wound Healing Society Symposium". *Advances in wound care, 2*(1), 1–4. https://doi.org/10.1089/wound.2012.0367. PMID: 24527316. PMCID: PMC3840478.

[51] Chung, J. Y., Chan, M. K., Li, J. S., et. al. (2021). "TGF- Signaling: From Tissue Fibrosis to Tumor Microenvironment". *International journal of molecular sciences ,22*(14), 7575. https://doi.org/10.3390/ijms22147575. PMID: 34299192. PMCID: PMC8303588.

[52] Abcam. *Generating cell knock-outs with CRISPR-Cas9 technology.* URL: https://www.abcam.com/reagents/generating-cell-knockouts-with-crispr-cas9-technology. (Accessed: 17.05.2022).

[53] Flouriot, G., Jehanno, C., Le Page, Y., et. al. (2020). "The Basal Level of Gene Expression Associated with Chromatin Loosening Shapes Waddington Landscapes and Controls Cell Differentiation". *Journal of molecular biology, 432*(7), 2253–2270. https://doi.org/10.1016/j.jmb.2020.02.016. PMID: 32105732.

[54] The Embryo Project Encyclopedia, Author: Zou, Y. (2014). *"Green Fluorescent Protein"*. ISSN: 1940-5030. URL: http://embryo.asu.edu/handle/10776/7903. (last updated: 27.01.2022). (Accessed: 17.05.2022).

[55] ThermoFisher Scientific. *mCherry Polyclonal Antibody.* URL: https://www.thermofisher.com/antibody/product/mCherry-Antibody-Polyclonal/PA5-34974. (Accessed: 17.05.2022).

[56] InvivoGen Innovation within reach. *HEK-Blue™ Detection.* URL: https://www.invivogen.com/hek-blue-detection. (Accessed: 17.05.2022).

[57] InvivoGen Innovation within reach. *HCT-116-Dual™ Cells.* URL: https://www.invivogen.com/hct116-dual. (Accessed: 17.05.2022).

[58] Frantz, C., Stewart, K. M., Weaver, V. M. (2010). "The extracellular matrix at a glance". *Journal of cell science, 123*(Pt 24), 4195–4200. https://doi.org/10.1242/jcs.023820. PMID: 21123617. PMCID: PMC2995612.

[59] Invivogen Innovation within reach. *HEK-Blue™ mNOD1.* URL: https://www.invivogen.com/hek-blue-mnod1. (Accessed: 17.05.2022).

[60] Khan Academy. *The endomembrane system.* URL: https://www.khanacademy.org/science/ap-biology/cell-structure-and-function/cell-compartmentalization-and-its-origins/a/the-endomembrane-system. (Accessed: 17.05.2022).

[61] Ibidi cells in focus. *The Principle of Immunofluorescence Assays.* URL: https://ibidi.com/content/364-the-principle-of-immunofluorescence-assays. (Accessed: 17.05.2022).

[62] Scitable by nature EDUCATION, Author: Pray, L. A. (2008). *DNA Replication and Causes of Mutation.* URL: https://www.nature.com/scitable/topicpage/dna-replication-and-causes-of-mutation-409/. (Accessed: 17.05.2022).

[63] ThermoFisher Scientific. *Overview of Western Blotting.* URL: https://www.thermofisher.com/dk/en/home/life-science/protein-biology/protein-biology-learning-center/protein-biology-resource-library/pierce-protein-methods/overview-western-blotting.html. (Accessed: 17.05.2022).

[64] Antibodies-online.com. Author: Krammer, D. K. *Western Blotting (Immunoblot): Gel Electrophoresis for proteins.* URL: https://www.antibodies-online.com/resources/17/1224/western-blotting-immunoblot-gel-electrophoresis-for-proteins/. (Accessed: 17.05.2022).

[65] ThermoFisher Scientific. *Gene Expression Analysis and Real-Time PCR (qPCR) Information.* URL: https://www.thermofisher.com/dk/en/home/life-science/pcr/real-time-pcr/real-time-pcr-learning-center/gene-expression-analysis-real-time-pcr-information.html. (Accessed: 17.05.2022).

[66] ThermoFisher Scientific. *Real-Time PCR (qPCR) Basics.* URL: https://www.thermofisher.com/dk/en/home/life-science/pcr/real-time-pcr/real-time-pcr-learning-center/real-time-pcr-basics.html. (Accessed: 17.05.2022).

[67] Sannino, A., Madaghiele, M., Carrozzo, M., et. al. (2011) "Nerve Tissue Engineering" *Comprehensive Biomaterials.* pp. 435-453.

11 Appendices

11.1 SEAP assay

The results illustrated in figure 3A of the experiment were captured by measuring the absorbance of the solution in the wells at an OD of 620 nm. The absorbance was measured for all three biological replicates made for each solution as represented in Table 1. This experiment was done using HEK detection with three vehicle controls measured at an absorbance of 0,2594, 0,251, and 0,2465 with an average of 0,2552. The calculated average of the three biological replicates of vehicle control was subtracted from the induced samples (S100A4-Multimer and IL-1β) to obtain a more precise measurement of absorbance without background noise, as represented in Table 2A. Table 2B represents the calculated average of the three biological replicates of each solution with subtracted background noise as well as the standard deviations calculated from the values in Table 2A. The results recited in Table 2B were used to plot the bar chart in figure 3B, as demonstrated in the results section.

Table 1: Results portraying the measured absorbance of the three biological replicates of cells stimulated with S100A4-Multimer (5 µg/ml) and the positive control, IL-1β (0.62-50 ng/ml). The absorbance of the solutions in the wells was measured at an OD of 620 nm.

SEAP assay	Replicate	Replicate	Replicate
S100A4 5 µg/ml	0,2593	0,2542	0,2523
IL-1β 0.62 ng/ml	0,4537	0,4485	0,4405
IL-1β 1.85 ng/ml	0,8796	0,8532	0,8997
IL-1β 5.55 ng/ml	1,6051	1,8495	1,772
IL-1β 16.6 ng/ml	1,9807	2,1931	2,2185
IL-1β 50 ng/ml	2,2671	2,4353	2,405

Table 2: Table 2A represents the calculated background subtracted for three biological replicates of cells stimulated with S100A4-Multimer (5 μg/ml) and the positive control, IL-1β (0.62-50 ng/ml). Table 2B represents the calculated average of the three biological replicates with subtracted background noise. Additionally, Table 2B depicts the calculated standard deviations. Both the average as well as the standard deviations were determined by utilising the numbers portrayed in Table 2A.

2A)

Background substracted		
0,0041	-0,0010	-0,0029
0,1985	0,1933	0,1853
0,6244	0,5980	0,6445
1,3499	1,5943	1,5168
1,7255	1,9379	1,9633
2,0119	2,1801	2,1498

2B)

	Average	STD
S100A4 5 µg/ml	0,0001	**0,00362**
IL-1β 0.62 ng/ml	0,1924	**0,006649**
IL-1β 1.85 ng/ml	0,6223	**0,023321**
IL-1β 5.55 ng/ml	1,4870	**0,124895**
IL-1β 16.6 ng/ml	1,8756	**0,130581**
IL-1β 50 ng/ml	2,1139	**0,089653**

The calculated averages of the three biological replicates of cells stimulated with S100A4-Multimer (5 μg/ml) and the positive control IL-1β (0.62-50 ng/ml) with background noise subtracted, were found using the command AVERAGE in Excel. The standard deviations were obtained by utilising the values of absorbance read for the three biological replicates with background subtracted as demonstrated in Table 2A. Furthermore, the calculation was done by use of the command STDEV in Excel. The standard deviations are visualized in figure 3B, where the error bars indicate the standard deviations based on N=3.

11.2 Components for induction of SEAP

Calculations:

During the SEAP assay procedure multiple components were used for the induction: S100A4-Multimer (1.25 and 5μg/ml) and IL-1β (0.62-50 ng/ml) of the cells. The concentrations needed for the induction were calculated by using the formula:

$$C_1 \cdot V_1 = C_2 \cdot V_2 \tag{1}$$

The stock concentration of S100A4-Multimer (Arxx produced batch) was 2.7 mg/ml, which is equal to 2700 μg/ml (C_1). The working concentration (WC) of S100A4-Multimer that was needed to be obtained was 5 μg/ml, which when diluted 10-fold is equal to 50 μg/ml (C_2). The chosen final volume of S100A4 stock after dilution was 108 μl (V_2). In order to prepare the desired final volume of S100A4 after dilution, the needed volume of S100A4 stock (V_1) was calculated by isolating V_1 in equation 1:

$$V_1 = \frac{50\ \mu\text{g/ml} \cdot 108\ \mu\text{l}}{2700\ \mu\text{g/ml}} = 2\ \mu\text{l} \tag{2}$$

Therefore, 2 μl of S100A4 stock was needed to obtain the final working volume (V_2) of 108 μl. In order to establish the final working volume, 106 μl of DPBS without Ca^{2+}/Mg^{2+} were combined with 2 μl S100A4-Multimer. From the calculated final working volume (V_2), 20 μl were utilised per well prior to adding 180 μl of cells.

The stock concentration of IL-1β was 20 μg/ml, which is equal to 20.000 ng/ml (C_1). The ranging WC of IL-1β that was needed to be obtained was 0.62-50 ng/ml. The WC of IL-1β of 50 ng/ml will be utilised for the calculations, which when diluted 10-fold is equal to 500 ng/ml (C_2). The chosen final volume of IL-1β stock after dilution was 200 μl (V_2). In order to prepare the desired volume of IL-1β after dilution, the needed volume of IL-1β stock (V_1) was calculated by isolating V_1 in equation 1:

$$V_1 = \frac{500\ \text{ng/ml} \cdot 200\ \mu\text{l}}{20.000\ \text{ng/ml}} = 5\ \mu\text{l} \tag{3}$$

Therefore, 5 μl of IL-1β stock was needed to obtain the final working volume (V_2) of 200 μl. In order to establish the final working volume, 195 μl of DPBS with Ca^{2+}/Mg^{2+} were combined with 5 μl IL-1β. From the calculated final working volume (V_2), 20 μl were utilised per well prior to adding 180 μl of cells. Once, the highest WC was prepared, then a 1:3 dilution row was made to establish the remaining WCs utilised for the experimental procedure.

11.3 SEAP experiment

The experiment was completed in the same manner as the SEAP assay as described in Appendix 11.1. The results illustrated in figure 7A of the experiment were captured by measuring the absorbance of the solution in the wells at an OD of 620 nm. The absorbance was measured for all three biological replicates made for each solution as represented in Table 3. Table 3 represents the data collected for the wells containing HCT-116 Dual RAGE 1. This experiment was done using HEK detection with three vehicle controls measured at an absorbance of 0.3077, 0.3139, and 0.03209 with an average of 0.3108. The calculated average of the three biological replicates of vehicle control was subtracted from the induced samples (S100A4-Multimer and IL-1β) to obtain a more precise measurement of absorbance without background noise as represented in Table 4A. Table 4B represents the calculated average of the three biological replicates of each solution with subtracted background noise as well as the standard deviations calculated from the values in Table 4A. The results recited in Table 4B were used to plot the bar chart in figure 7B, as demonstrated in the results section.

The calculated averages of the three biological replicates of cells stimulated with S100A4-Multimer (1.25 μg/ml and 5 μg/ml) and the positive control IL-1β (0.62-16.6 ng/ml) with background noise subtracted, were found using the command AVERAGE in Excel. The standard deviations were obtained by utilising the values of absorbance read for the three biological replicates with background subtracted as demonstrated in Table 4A. Furthermore, the calculation was done by use of the command STDEV in Excel. The standard deviations are visualized in figure 7B, where the error bars indicate the standard deviations based on N=3.

The experiment established was duplicated for the wells containing HCT-116 Dual RAGE 3, and the data collected is represented in Tables 5 and 6, respectively.

Table 3: Results portraying the measured absorbance of the three biological replicates of HCT-116 Dual RAGE 1 stimulated with S100A4-Multimer (1.25 μg/ml and 5 μg/ml) and the positive control, IL-1β (0.62-16.6 ng/ml). The absorbance of the solutions in the wells was measured at an OD of 620 nm.

SEAP assay	Replicate	Replicate	Replicate
S100A4 1.25 µg/ml	0,3156	0,3263	0,3137
S100A4 5 µg/ml	0,3186	0,3173	0,325
IL-1β 0.5 ng/ml	0,5414	0,5472	0,5431
IL-1β 1.6 ng/ml	0,8579	0,7705	0,8195
IL-1β 5 ng/ml	1,1056	1,086	1,2595
IL-1β 15 ng/ml	1,4942	1,4427	1,4614

Table 4: Table 4A represents the calculated background subtracted for three biological replicates of HCT-116 Dual RAGE 1, stimulated with S100A4-Multimer (1.25 µg/ml and 5 µg/ml) and the positive control, IL-1β (0.62-16.6 ng/ml). Table 4B represents the calculated average of the three biological replicates with subtracted background noise. Additionally, Table 4B depicts the calculated standard deviations (STD). Both the average as well as the standard deviations were determined by utilising the numbers portrayed in Table 4A.

4A)

Background substracted		
0,0048	0,0155	0,0029
0,0078	0,0065	0,0142
0,2306	0,2364	0,2323
0,5471	0,4597	0,5087
0,7948	0,7752	0,9487
1,1834	1,1319	1,1506

4B)

	Average	STD
S100A4 1.25 µg/ml	0,0077	**0,00757**
S100A4 5 µg/ml	0,0095	**0,00092**
IL-1β 0.62 ng/ml	0,2331	**0,0041**
IL-1β 1.85 ng/ml	0,5052	**0,0618**
IL-1β 5.55 ng/ml	0,8396	**0,01386**
IL-1β 16.6 ng/ml	1,1553	**0,03642**

Table 5: Results portraying the measured absorbance of the three biological replicates of HCT-116 Dual RAGE 3 stimulated with S100A4-Multimer (1.25 µg/ml and 5 µg/ml) and the positive control, IL-1β (0.62-16.6 ng/ml). The absorbance of the solutions in the wells was measured at an OD of 620 nm.

SEAP assay	Replicate	Replicate	Replicate
S100A4 1.25 µg/ml	0,3252	0,3196	0,3175
S100A4 5 µg/ml	0,3434	0,3195	0,3097
IL-1β 0.5 ng/ml	0,6074	0,604	0,6
IL-1β 1.6 ng/ml	0,9481	0,8485	0,9319
IL-1β 5 ng/ml	1,2584	1,1847	1,2032
IL-1β 15 ng/ml	1,3706	1,3592	1,3631

Table 6: Table 6A represents the calculated background subtracted for three biological replicates of HCT-116 Dual RAGE 3 stimulated with S100A4-Multimer (1.25 µg/ml and 5 µg/ml) and the positive control, IL-1β (0.62-16.6 ng/ml). Table 6B represents the calculated average of the three biological replicates with subtracted background noise. Additionally, Table 6B depicts the calculated standard deviations (STD). Average and standard deviations were determined by utilising the numbers portrayed in Table 6A.

6A)

Background substracted		
-0,0068	-0,0124	-0,0145
0,0114	-0,0125	-0,0223
0,2754	0,2720	0,2680
0,6161	0,5165	0,5999
0,9264	0,8527	0,8712
1,0386	1,0272	1,0311

6B)

	Average	STD
S100A4 1.25 µg/ml	-0,0112	**0,00398**
S100A4 5 µg/ml	-0,0078	**0,01733**
IL-1β 0.62 ng/ml	0,2718	**0,0037**
IL-1β 1.85 ng/ml	0,5775	**0,05344**
IL-1β 5.55 ng/ml	0,8834	**0,03834**
IL-1β 16.6 ng/ml	1,0323	**0,00579**